Origin of the Tongbai-Dabie-Sulu Neoproterozoic low-$\delta^{18}O$ igneous province, east-central China

Bin Fu [1] *, Noriko T. Kita [2], Simon A. Wilde [3], Xiaochun Liu [4], John Cliff [5], Alan Greig [1]

[1] School of Earth Sciences, The University of Melbourne, Parkville, VIC 3010, Australia

[2] WiscSIMS, Department of Geoscience, University of Wisconsin, Madison, WI 53706, USA

[3] Department of Applied Geology, Curtin University, Perth, WA 6102, Australia

[4] Institute of Geomechanics, Chinese Academy of Geological Sciences, Beijing, 100081, PR China

[5] Centre for Microscopy, Characterisation and Analysis, The University of Western Australia, Crawley, WA 6009, Australia

* Corresponding author. E-mail address: binfu@unimelb.edu.au

Running title: Orign of the Tongbai-Dabie-Sulu Neoproterozoic Igneous Province

Resubmitted to *Contributions to Mineralogy and Petrology*

27th October 2012

Abstract

Zircons from 71 diverse rocks from the Qinling-Tongbai-Dabie-Sulu orogenic belt in east-central China and, for comparison, 8 from adjoining areas in the South China and North China blocks, have been analyzed for in situ $^{18}O/^{16}O$ ratio and/or U-Pb age to further constrain the spatial distribution and genesis of Neoproterozoic low-$\delta^{18}O$ magmas, i.e. $\delta^{18}O(zircon) \leq 4‰$ VSMOW. In many metaigneous rock samples from Tongbai-Dabie-Sulu, including high-pressure and ultrahigh-pressure eclogites and associated granitic orthogneisses, average $\delta^{18}O$ values for Neoproterozoic "igneous" zircon cores (i.e. 800 to 600 Ma) vary from –0.9‰ to 6.9‰, and from –9.9‰ to 6.8‰ for Triassic metamorphic rims (i.e. 245 to 200 Ma). The former extend to values lower than zircons in primitive magmas from the Earth's mantle (ca. 5‰ to 6‰). The average $\Delta^{18}O$ (metamorphic zircon – "igneous" zircon) values vary from –11.6‰ to 0.9‰. The large volume of Neoproterozoic low-$\delta^{18}O$ igneous protoliths at Tongbai-Dabie-Sulu is matched only by the felsic volcanic rocks of the Snake River Plain hotspot track, which terminates at the Yellowstone Plateau. Hence, the low-$\delta^{18}O$ values at Tongbai-Dabie-Sulu are proposed to result from shallow sub-caldera processes by comparison with Yellowstone, where repeated caldera-forming magmatism and hydrothermal alteration created similar low-$\delta^{18}O$ magmas. However, the possibility of involvement of meltwaters from local continental glaciations, rather than global Neoproterozoic glaciations, cannot be precluded. Our data indicate that Neoproterozoic low-$\delta^{18}O$ magmas that are either subduction- or rift-related, are present locally along the western margin of the South China Block (e.g. Baoxing Complex). It appears that Neoproterozoic ^{18}O-depletion events in the South China Block as the result of hydrothermal alteration and magmatism affected a much larger area than was previously recognized.

Keywords

Zircon, Oxygen isotopes, Ultrahigh-pressure metamorphism, Qinling-Tongbai-Dabie-Sulu orogenic belt, South China Block

INTRODUCTION

Zircon may preserve pristine igneous structures and compositions even in highly metamorphosed or hydrothermally altered rocks including: oscillatory zoning as revealed by scanning electron microscopy – cathodoluminescence (SEM-CL) imaging, magmatic ages and chemical and/or isotopic compositions (e.g. Ti, REE – rare earth elements, Hf, Th, U, O). Thus zircons provide unique information (e.g. age, fluid-rock interaction, temperature, and source) about the protolith or host rocks and their tectonic environment. For instance, the measured $\delta^{18}O$ values of igneous zircons commonly represent the oxygen isotope composition during crystallization of the magma (e.g. Lancaster et al. 2009; Fu et al. 2012). Post magmatic exchange is retarded due to the slow diffusion of oxygen isotopes at crustal temperatures and recrystallization as a result of metamorphism can be evaluated by U-Pb geochronology (e.g. Valley et al. 1994; Watson and Cherniak 1997; Valley 2003; Zheng et al. 2004; Page et al. 2007a; Bowman et al. 2011). Furthermore, oxygen isotope zoning within single igneous zircons (e.g. core-rim structure) provides critical evidence to decipher complex overprinting events of magmatism and hydrothermal alteration (e.g. Bindeman et al. 2008a; Chen et al. 2011). A rapidly growing number of in situ oxygen isotope studies of zircons with ages from 4.4 Ga to <1 Ma in diverse rock types have been carried out by ion microprobe (secondary ion mass spectrometry, SIMS) to determine the evolution of the early Earth and later magmatism and metamorphism (e.g. Cavosie et al. 2005; Kemp et al. 2007; Trail et al. 2007; Harrison et al. 2008; Ickert et al. 2008; Grimes et al. 2011; Chen et al. 2011; Dai et al. 2011; Jeon et al. 2012).

Zircons in granitic orthogneisses associated with high- and ultrahigh-pressure (HP/UHP) eclogites from the Dabie-Sulu orogenic belt, eastern China, have a wide range in average $\delta^{18}O$ values from –9.0‰ to 6.2‰ VSMOW (e.g. Rumble et al. 2002; Zheng et al. 2004; Tang et al. 2008a,b). Low $\delta^{18}O(Zrn)$ in these rocks has been attributed to high-temperature exchange between Neoproterozoic igneous protoliths and isotopically light glacier melt-water during the Neoproterozoic glacial events (i.e. including the "snowball Earth") (e.g. Rumble et al. 2002; Zheng et al. 2004, 2008). SIMS analyses of "igneous" zircon cores and so-called "metamorphosed" zircons in the eclogites and granitic orthogneisses indicate that $\delta^{18}O(Zrn)$ varies from 0.1‰ to 10.1‰ (e.g. Chen et al. 2003,

2011). As discussed in detail by Wu et al. (2007), high-temperature hydrothermal alteration of the Middle Neoproterozoic igneous rocks at Dabie resulted in low and negative $\delta^{18}O$ values for rock-forming minerals, and some of the altered rocks were locally melted to generate low-$\delta^{18}O$ magmas. Furthermore, the ^{18}O-depletion events took place at 780-740 Ma and so they clearly predate the "snowball Earth" events (i.e. Sturtian & Marinoan) between 720 Ma and 635 Ma (Zheng et al. 2007a, 2008 and references therein). Alternative explanations have also been discussed by Wang et al. (2011a) and Bindeman (2011). Thus, it appears that the occurrence of low-$\delta^{18}O$ magmas in the South China Block during the Neoproterozoic may be unrelated to global glaciation events.

Numerous U-Pb zircon ages obtained by ID-TIMS (isotope dilution – thermal ionization mass spectrometry), SIMS and LA-ICP-MS (laser ablation – inductively coupled plasma mass spectrometry) for rocks from the Tongbai-Dabie-Sulu orogenic belt have been published and many of the U-Pb zircon age data were summarized in Zheng et al. (2003, 2008, 2009). In this contribution, we employed CAMECA IMS-1280 ion microprobes, combined with SIMS/LA-ICP-MS U-Pb dating, in order to obtain precise and accurate in situ analyses of oxygen isotope ratios in igneous and/or metamorphic zircons in diverse rocks obtained throughout the Tongbai-Dabie-Sulu orogenic belt, east-central China; we also included samples from adjacent areas in the South China and North China blocks for comparative purposes. The goal of this study was to further constrain the spatial distribution and genesis of low-$\delta^{18}O$ magmas in the Tongbai-Dabie-Sulu orogenic belt, and to determine its tectonic, magmatic, and hydrothermal history prior to the Triassic HP/UHP eclogite-facies metamorphism.

GEOLOGICAL SETTING AND SAMPLE DESCRIPTIONS

The Triassic continental collision between the North China Block and the South China Block in east-central China has generated the most extensive HP/UHP metamorphic province in the world. These rocks are exposed in the southern and eastern parts of the Qinling-Tongbai-Dabie-Sulu orogenic belt in a terrane extending >1500 km from west to east (inset of Fig. 1a). The most notable terranes are, from west to east, Tongbai, Hong'an (West Dabie), Dabie and Sulu, which were

105 disrupted by three major NNE-SSW trending faults, the Dawu and the Shangcheng-Macheng faults
106 (DF & SMF; Fig. 1b) and the Tancheng-Lujiang or Tan-Lu Fault (TLF; Figs. 1a & 1b). These terranes
107 expose a coherent sequence of subducted continental crust and cover now exhumed at the surface.
108 The Hong'an, Dabie and Sulu terranes contain both HP and UHP units, which were intruded by
109 massive post-orogenic Cretaceous granites and minor mafic-ultramafic complexes. The UHP units
110 consist of abundant ortho- and paragneiss, schist, marble, jadeite/kyanite quartzite and minor eclogite
111 lenses and garnet-bearing ultramafic complexes. The HP units mainly consist of gneiss, amphibolite,
112 and eclogite. Coesite inclusions have been reported in zircons obtained from eclogites, particularly
113 from associated gneisses (e.g. Ye et al. 2000; Liu et al. 2002; Liu and Liou 2011).
114 The Sulu terrane is bounded to the northwest by the Jiaobei terrane of the North China Block
115 along the Wulian-Yantai Fault (WYF) and to the southeast by the South China Block along the
116 Jiashan-Xiangshui Fault (JXF) (Fig. 1a). Rocks of the HP unit in the Sulu terrane occur sporadically
117 south-east of the UHP unit. The Precambrian basement in the Jiaobei terrane consists of Archean
118 tonalite-trondhjemite-granodiorite (TTG) and supracrustal rocks including banded iron formation
119 (BIF), and Palaeoproterozoic amphibolite and granulite (Tang et al. 2007; Zhou et al. 2008 and
120 references therein).
121 The Dabie terrane is divided into five lithotectonic units by E-W-trending faults, including the
122 Xiaotian-Mozitan Fault, the Wuhe-Shuihou Fault (shear zone), the Hualiangting-Mituo Fault and the
123 Taihu-Shanlong Fault (XMF, WSF, HMF & TSF in Fig. 1b; Liu et al. 2007). From north to south,
124 these units are (Zheng et al. 2008 and references therein): (I) the Beihuaiyang low-T/low-P
125 greenschist-facies unit; (II) the North Dabie high-T/UHP granulite-facies unit; (III) the Central Dabie
126 middle-T/UHP eclogite-facies unit; (IV) the South Dabie low-T/UHP eclogite-facies unit; and (V) the
127 Susong low-T/high-P blueschist-facies unit (Fig. 1b).
128 In the Hong'an terrane, there are six lithotectonic units from north to south (Liu et al. 2004):
129 (A) the Nanwan meta-flysch unit; (B) the Balifan mélange; (C) the Huwan HP unit; (D) the Xinxian
130 UHP unit; (E) the Hong'an HP unit; and (F) the Mulanshan blueschist unit (Fig. 1b). The Nanwan
131 flysch unit is composed of Devonian bedded quartz sandstone, pelite and greywacke and all the rocks
132 are metamorphosed to greenschist or epidote-amphibolite facies. The Balifan tectonic mélange unit

consists of augen mylonite, mylonitized quartzofeldspathic schist and epidote amphibolite with many large metagabbro blocks. The Huwan HP unit compromises augen gneiss, mylonite, quartzofeldspathic schist, graphite schist and marble with numerous eclogite blocks. The Xinxian UHP is a structural dome composed of granitic to granodioritic gneiss and minor supracrustal rock with abundant eclogite lenses or pods. The Hong'an HP unit consists of quartzofeldspathic schist, granitic orthogneiss, marble, quartzite and graphite schist with layered garnet amphibolite, as well as eclogite and ultramafic blocks or lenses. The Mulanshan blueschist-greenschist unit is mainly composed of felsic and mafic volcanic rocks associated with metasedimentary phosphorite, graphite schist and quartzite in the lower part, and metapelite and marble in the upper part.

The Tongbai terrane represents the middle segment of the Qinling-Tongbai-Dabie-Sulu orogenic belt. It is separated from Qinling in the west by the Nanyang Basin, and from Hong'an in the east by the Dawu Fault. The terrane comprises six collision-related lithotectonic units, separated by large-scale shear zones (Liu et al. 2008, 2010a). From northeast to southwest, they are: (1) the Nanwan flysch, (2) the Balifan tectonic mélange, (3) the northern eclogite zone, (4) the Tongbai Complex, (5) the southern eclogite zone, and (6) the blueschist-greenschist zone (Fig. 1c). A coesite-bearing eclogite zone is however absent. Eclogites from the two eclogite zones commonly occur as lenses or blocks of a few to several hundreds meters in size in quartzofeldspathic gneisses, mica schists and marbles. The Tongbai Complex is dominated by coarse-grained gneissic granites. Most of these rocks were strongly deformed and commonly converted to augen gneisses and mylonites. The enclaves in the gneissic and weakly foliated granites comprise fine-grained dioritic-trondhjemitic gneisses and minor amphibolites, paragneisses, calc-silicates and marbles. The dioritic-trondhjemitic gneisses are layered and commonly show granitic and pegmatitic veins. Amphibolites occur as interlayers or lenses within the dioritic-trondhjemitic gneisses.

The Baoxing Complex is located in the southern Longmen Shan, while the Pengguan and Xuelongbao complexes lie to the north, between the Tibet Plateau and the Sichuan Basin in southwestern China (Fig. 1d). It consists mainly of highly deformed mafic to felsic (gabbroic, dioritic, tonalitic, granodioritic and monzogranitic) gneisses. The Neoproterozoic igneous rocks were emplaced into the Yanjing Group that is composed of an intermediate-acidic to alkaline volcanic

complex, pelitic clastic rocks, and carbonates (BGMRSP 1991). The cover sequences in this area include a thin, incomplete succession of Neoproterozoic to Middle Triassic shallow-marine and nonmarine sedimentary rocks (Burchfiel et al. 1995). All the Precambrian basement rocks and the cover sequences were folded/deformed and metamophised to greenschist to amphibolite-facies during the early Mesozoic. The massive tonalitic gneiss consists mainly of plagioclase, quartz, biotite and minor amphibole and K-feldspar.

Zircons from 71 samples were chosen for analysis (Fig. 1): 17 samples from Sulu; 10 from Dabie; 18 from Hong'an; 23 from Tongbai; and 3 from South Qinling (e.g. Hannan Massif). The majority of the investigated samples are metaigneous rocks, including metagabbro, HP/UHP eclogite, garnet amphibolite and granitic (or dioritic/trondjiemitic/quartzofeldspathic) orthogneiss from different lithotectonic units in the four terranes of the Tongbai-Dabie-Sulu orogenic belt. Metasedimentary rocks including paragneiss, schist, quartzite and felsic granulite that may contain detrital zircons, as well as pre-orogenic intrusions, syn-orogenic (Triassic) pegmatitic dikes (Wallis et al. 2005) and post-orogenic Cretaceous intrusions (Liu et al. 2010a; Cui et al. 2012) were selected for comparison (Electronic supplementary materials or ESM S1). In addition, 6 samples from southern Longmenshan (Baoxing Complex) and Yichang (Huangling Granitoid) in the South China Block and 2 samples from the southern margin of the North China Block were also analyzed.

ANALYTICAL METHODS

For some samples, oxygen isotope analyses of garnet, amphibole, zoisite and/or quartz were performed in bulk on 1-2 milligram-size samples using laser fluorination (λ = 10.6 μm, BrF_5) and gas-source mass-spectrometry at the University of Wisconsin – Madison (Valley et al. 1995). The $^{18}O/^{16}O$ ratios are reported in δ notation relative to Vienna Standard Mean Ocean Water (VSMOW). All $\delta^{18}O$ values were corrected using the accepted values of the standards employed: 5.80‰ for UWG-2, Gore Mountain garnet standard (Valley et al. 1995) and 9.59‰ for NBS-28 quartz standard, and they are tabulated in Electronic ESM S2. All the data are reported here with uncertainty within 2 standard deviations (2 SD) or at the 95% confidence levels (c.l.).

Zircon separates were obtained by standard crushing, magnetic, and heavy liquid techniques, and were then handpicked under a binocular microscope. Unknown zircon (and quartz) grains together with zircon standards (KIM-5, CZ3, Temora-2, and/or Plešovice) (and quartz standard, UWQ-1) were cast in epoxy, ground, and polished to expose the midsection of the grains. Nine 25mm round zircon grain mounts were prepared, together with 11 other mounts previously prepared for in situ U-Pb zircon dating by ion microprobe (Liu et al. 2004, 2008, 2010a; Wallis et al. 2005; Cui et al. 2012; Hu et al. 2012); some of the mounts were face-mounted with KIM-5 or Plešovice in the center and many of the previous geochronology pits were ground off.

Secondary electron and cathodoluminescence imaging of the zircons was conducted using a Hitachi S-3400N scanning electron microscope at the University of Wisconsin – Madison or a Philips (FEI) XL30 ESEM (environmental SEM) at the University of Melbourne, both equipped with a Gatan CL detector. Representative CL images of the zircons of interest are shown in Fig. 2 and indicate that many zircons display core–rim structures: Zircon cores commonly exhibit oscillatory zoning in CL, whereas zircon rims tend to be weakly zoned or featureless.

Ion microprobe analyses of $^{18}O/^{16}O$ ratios in zircons were conducted using 10-15 micron spots on a CAMECA IMS-1280 ion microprobe with multi-collector Faraday Cups (FC) at the WiscSIMS center at the University of Wisconsin – Madison (Kita et al. 2009). Ion microprobe analyses of $^{18}O/^{16}O$ ratios in zircons and quartz grains were also performed on a CAMECA IMS-1280 ion microprobe at the University of Western Australia; analytical procedures and data reduction were similar to those reported in Kita et al. (2009). All oxygen isotope results on samples and standards including KIM-5 ($\delta^{18}O$ = 5.09±0.12‰; Valley 2003), Plešovice (8.19±0.08‰; J.W. Valley unpublished data), Temora-1 (7.93±0.08‰; Valley 2003; Black et al. 2004); and Temora-2 (8.20±0.02‰; Valley 2003; Black et al. 2004) as well as UWQ-1 (quartz, 12.33±0.14‰; Kelly et al. 2007), are listed in order of analysis in ESM S3. Optical microscope photographs of the oxygen isotope SIMS spots were taken and digitized and/or post-analysis SEM imaging of many of the SIMS spots was performed to evaluate the reliability of in situ ion microprobe data.

After grinding off previous SIMS spots for $^{18}O/^{16}O$ ratio, the U, Th, and Pb compositions and U–Pb isotopic ratios for some of the zircons were obtained from newly-polished, gold-coated zircon grain mounts using a SHRIMP II ion microprobe at the John de Laeter Centre of Mass Spectrometry, Curtin University, Perth. The operating conditions and analytical protocols using seven-cycle runs through the mass stations are essentially the same as described by Williams (1998). The SHRIMP spots were ca. 25 µm in diameter. The Pb/U calibration was performed using the in-house CZ3 standard zircon ($^{206}Pb/^{238}U$ age = 564 Ma; Pidgeon et al. 1994), which was analyzed repeatedly throughout each session. All raw SIMS data files were reduced using the Squid program (Ludwig 2001a), and relative probabilities plotted using Isoplot/Ex (Ludwig 2001b). Apparent ages include uncertainty in the Pb/U calibration, and all errors are quoted at 2 SE (standard error) precision (ESM S4). Four zircon grains from sample 26 (Mount G72) were analyzed for U–Th–Pb isotopes using a SHRIMP II ion microprobe at the Institute of Geology, Chinese Academy of Geological Sciences, Beijing (cf. Liu et al. 2004).

Laser ablation U-Th-Pb isotope analyses of many of the studied zircons were carried out at the University of Melbourne, using a 193 nm excimer laser-based HELEX ablation system equipped with a Varian 810 quadrupole ICP-MS described in Woodhead et al. (2004, 2007) and Paton et al. (2010) and also using an Agilent 7700 ICP-MS. U-Th-Pb isotopic abundances were analysed using a 32 µm spot size. All data manipulation was done offline using the locally developed Iolite software package (Hellstrom et al. 2008) with the U-Th-Pb data reduction module of Paton et al. (2010). The results were calibrated with the 91500 zircon (Wiedenbeck et al. 1995) as the primary standard and are tabulated in ESM S5, and the weighted mean $^{206}Pb/^{238}U$ ages obtained from two secondary standard zircons Temora-2 (415.9 ± 1.1 Ma, n=54; 419.2 ±1.4 Ma, n=68) and Plešovice (338.8 ± 0.9 Ma, n=33; 339.4 ± 0.7 Ma, n=90) in two sessions and are well within ±1.0% of the accepted ages (416.8 Ma & 337.1 Ma: Black et al. 2004; Sláma et al. 2008).

The initial common Pb isotopic composition of the analyzed zircons from different rocks was estimated using the two-stage terrestrial Pb evolution model of Stacey and Kramers (1975) at a given age; however, only radiogenic $^{207}Pb/^{206}Pb$ ages for zircons older than 1.2 Ga are presented.

OXYGEN ISOTOPE COMPOSITIONS

Laser Fluorination Bulk Analyses

Mineral separates analyzed by laser fluorination are from HP/UHP eclogites and jadeite quartzite at Dabie-Sulu (ESM S2). Garnet from the HP/UHP eclogites has a large range in $\delta^{18}O$ from –8.1‰ to 9.4‰.

Coexisting minerals were analyzed in order to determine the extent of isotopic disequilibrium and fluid-'buffered' open system exchange (i.e. Valley 2001; Zheng et al. 2003). For an individual rock sample, compared to garnet, the coexisting omphacite, amphibole and zoisite commonly have a slightly higher $\delta^{18}O$ value, as evident by positive $\Delta^{18}O(Min - Grt)$ values, ranging between 0.17‰ and 0.86‰ (Fig. 3). Here, $\Delta^{18}O(Min - Grt) = \delta^{18}O(Min) - \delta^{18}O(Grt)$ and Min stands for omphacite, zoisite, or amphibole and Grt for garnet. Oxygen isotope fractionation between omphacite ($diopside_{40}$ - $jadeite_{60}$), zoisite or amphibole (glaucophane) and garnet at T = 700ºC (or higher) using the calibrations of Zheng (1993a,b) is estimated to be ca. 1‰ or less. Within the accuracy of these estimates, the small oxygen isotope fractionations measured between these minerals suggest that the value for high temperature isotopic equilibrium has been attained and preserved at peak-HP/UHP metamorphic conditions (e.g. Yui et al. 1995; Zheng et al. 1996, 1998a, 2003; Baker et al. 1997; Rumble and Yui 1998).

Ion Microprobe Spot Analyses

Results of all SIMS spot analyses of unknown zircons are shown in Fig. 4 and individual $\delta^{18}O$ data for all the investigated samples are summarized in ESM S1. Nine analyses of 7 quartz grains from one granitic orthogneiss sample (#6) that are not shown in Fig. 4 give a narrow range in $\delta^{18}O$ from –1.9‰ to –1.3‰, averaging –1.6±0.4‰.

The lowest $\delta^{18}O$ value for zircon is –10.8‰ from one UHP eclogite sample (#2), and the highest $\delta^{18}O$ value is 13.8‰ from one HP eclogite sample (#47) and one Paleoproterozoic pelitic schist sample (#50).

Zircons from some metaigenous or igneous rock samples, especially from Hong'an and Tongbai (e.g. #33, #40 & #69), have a narrow range in $\delta^{18}O$, varying by only 0.2‰ to 0.8‰ (Fig. 4). This indicates $^{18}O/^{16}O$-homogeneity in zircons at hand specimen scale. The intergrain variability can also be evaluated by a 2 SD value of average $\delta^{18}O$(Zircon) or $\delta^{18}O$(Zrn) for some invididual rock samples (e.g. ±0.1‰ to ±0.5‰; ESM S1), comparable to the analytical precision of ±0.4‰. On the other hand, $\delta^{18}O$ in zircons from some other granitic orthogneiss/eclogite samples, notably from Dabie and Sulu (e.g. #2), can be highly variable by up to 20.4‰. The 2 SD value of the average $\delta^{18}O$(Zrn) for the metaigneous rocks is as high as ±7.0‰ (#47) and ±9.1‰ (#20). It is noted that the 2 SD value of the average $\delta^{18}O$(Zrn) for most invididual samples other than eclogites and orthogneisses is ±2.2‰ or less. Many zircons from metaigenous rocks have much higher $\delta^{18}O$ values in the core than the rim (Figs. 2a to c). Since the distinction between "igneous" zircons and "metamorphic" zicons is not always straightforward, intragrain and intergrain variability in $\delta^{18}O$ was based on CL images and U-Th-Pb results and is assessed in the Discussion section.

Average $\delta^{18}O$(Zrn) values for the investigated rocks at Qinling-Tongbai-Dabie-Sulu vary from –7.4‰ to 13.3‰ (ESM S1). In detail, average $\delta^{18}O$(Zrn) values for metaigneous rocks can be highly variable: 3.6‰ and 4.7‰ for metagabbros; from –7.4‰ to 10.0‰ for eclogites; from 3.0‰ to 6.7‰ for garnet amphibolites; and from –3.7‰ to 5.4‰ for orthogneisses, including one leucosome sample (#53). In contrast, there is a narrow range in $\delta^{18}O$(Zrn) for the granitic intrusions: from 3.5‰ to 4.5‰ for pegmatites and from 5.0‰ to 5.6‰ for granites and granodiorites. Zircons in paragneisses, quartzites, felsic granulites and pelitic schists have average $\delta^{18}O$ values between 5.3‰ and 13.3‰. Overall, zircons have average $\delta^{18}O$ values, from –7.4‰ to 6.8‰ for the 17 samples from Sulu; from –3.6‰ to 7.5‰ for the Dabie samples (10); from –3.3‰ to 10.0‰ for samples from Hong'an (18); and –1.1‰ to 13.3‰ for the Tongbai samples (23). Average $\delta^{18}O$(Zrn) values for three samples (#70-72) from South Qinling vary from 6.8‰ to 8.5‰.

By comparison, many zircons in samples (#73-77) from the Baoxing Complex of southern Longmenshan in the South China Block are characterized by oscillatory zonation typical of igneous zircons as revealed by CL imaging. Some zircons in sample #76 display core-rim structure and the

297 zircon rims are featureless. Spot analysis of twenty-three zircon grains in four metagranite samples
298 (#74-77) indicates a large variation in $\delta^{18}O$ of between 1.9‰ and 9.9‰ (Fig. 4). Average $\delta^{18}O$ values
299 for the Baoxing samples range from 4.0‰ to 6.7‰ (ESM S1). One metarhyolite sample (#73) from
300 the Yanjing Group in the same area has an average $\delta^{18}O$(Zrn) value as low as 3.9±0.9‰. Zircon $\delta^{18}O$
301 for one sample (#78), also from the Huangling granitoid in the South China Block, varies from 6.6‰
302 to 8.8‰, averaging 7.9±1.8‰.
303 Zircons in two samples (#18 & #79) from the North China Block have an average $\delta^{18}O$ value
304 of 5.7±0.5‰ and 5.9±0.4‰, respectively (ESM S1).
305
306 **IN SITU U-Pb GEOCHRONOLOGY**
307 Sixty-four out of 65 SIMS U-Th-Pb analyses of selected zircons from 19 samples from
308 Dabie-Sulu indicate that there are two major $^{206}Pb/^{238}U$ age populations (Fig. 5a & ESM S4): (1) at
309 205 to 246 Ma (n=22) for metamorphic zircon rims (Th/U < 0.3) and (2) 606 to 797 Ma (n=27) for
310 igneous zircon cores (Th/U > 0.3).
311 U-Th-Pb analysis of zircons from 49 samples by LA-ICP-MS was carried out in two separate
312 sessions (ESM S5) to determine the (re-)crystallisation age of the zircons and data for 5 representative
313 samples were plotted on concordia diagrams (Figs. 5b to 5f). At Tongbai-Dabie-Sulu, zircons in 8 out
314 of 10 eclogite samples give Neoproterozoic ages for the igneous protoliths, and Triassic ages for the
315 rims that resulted from syn-orogenic HP/UHP metamorphism. Zircons in one UHP eclogite sample
316 (#19) from Dabie give discordia intercept ages of 1924±17 Ma and 231±15 Ma (Fig. 5b), whereas
317 metamorphic zircons in one HP eclogite sample (#30) from Hong'an give a weighted mean age of
318 305±5 Ma (n=9) (Fig. 5c). Likewise, zircons in 17 out of the 21 orthogneiss samples analyzed give
319 Neoproterozoic protolith ages and Triassic rim ages that record syn-orogenic HP/UHP metamorphism
320 (e.g. Fig. 5d). A few small igneous zircons (or cores) in 4 orthgneiss samples (#11, #25, #37 & #39)
321 give younger Paleozoic ages. Nevertheless, discordia upper intercept ages of 771±86 Ma and 752±70
322 Ma on the concordia diagrams are obtained for both UHP eclogite and granitic orthogneiss samples
323 from the same location (#37 & #39) (Wu et al. 2008a).

Zircons in one granite sample (#26) from Dabie give a weighted mean age of 752±4 Ma (n=45) (Fig. 5e), whereas zircons in a granodiorite sample (#69) from Tongbai give a weighted mean age of 454±6 Ma (n=12). The latter reflects the timing of arc magmatism in the region (e.g. Wang et al. 2011b).

Archean to Paleoproterozoic zircons have been preserved in paragneiss (#9), quartzite (#23) and felsic granulite (#27), whereas no zircons older than 600 Ma were determined in one paragneiss sample (#22). Zircons in a paragneiss sample (#28) from a Cretaceous dome at Dabie are as old as 3.0 Ga (ESM S1).

Zircons in samples from South Qinling and the South China Block (#70-78) give a weighted mean $^{206}Pb/^{238}U$ age or a discordant intercept age varying from 896 Ma to 775 Ma, reflecting the timing of magmatism (ESM S1; see Fig. 5f for #77). In contrast, zircons in two samples (#18 & #79) from the North China Block give a much older age, 2.91 Ga for magmatism and 1.84 Ga for metamorphism.

DISCUSSION

Based on CL images and available U-Th-Pb data, we first attempt to distinguish Neoproterozoic "igneous" zircons from Triassic "metamorphic" zircons in the investigated rocks at Tongbai-Dabie-Sulu. We then investigate the origin of low-$\delta^{18}O$ Neoproterozoic igneous zircons or host igneous rocks in the region, using a comparison with Yellowstone caldera, USA, where similar oxygen signatures have been obtained. Finally, the geological implications of $\delta^{18}O$ for zircons of Archean to Cretaceous ages are discussed.

"Metamorphic" Zircon *versus* "Igenous" Zircon

Both SIMS U-Th-Pb results (Liu et al. 2004, 2008, 2010a; Wallis et al. 2005; Cui et al. 2012; Hu et al. 2012; this study) and LA-ICP-MS U-Th-Pb results were plotted against SIMS $\delta^{18}O$ data for all zircon samples of this study from the Tongbai-Dabie-Sulu orogenic belt, including South Qinling, and from the South China and North China blocks (Fig. 6a). While both datasets are largely

351 comparable, LA-ICP-MS age estimatess are much younger or older than SIMS ages for a few zircons
352 (ESM S6). In this case, SIMS ages are preferred due to very small volume of material analysed,
353 comparable with SIMS $\delta^{18}O$ spots (cf. Chen et al. 2011; Sheng et al. 2012).

354 In general, Archean and Paleoproterozic zircons have $\delta^{18}O$ values varying from 3.6‰ to
355 13.8‰, whereas younger zicons of Mesoproterozoic to Cretaceous age have a wide range in $\delta^{18}O$
356 between –10.8‰ and 12.0‰. It is noted that many Paleoproterozoic and Triassic zircons that have
357 extremely low or high $\delta^{18}O$ values also have lower Th/U values than other zircons (see inset of Fig.
358 6a).

359 For many zircons from the Tongbai-Dabie-Sulu HP/UHP metamorphic rocks, the distinction
360 between igneous cores and metamorphic rims may be verified because the cores commonly have
361 higher Th/U ratios and give older U-Pb ages than the rims (e.g. Zheng et al. 2004; Chen et al. 2006).
362 However, this may not always be the case, especially for those so-called "metamorphosed" protolith
363 zircons variably recrystallized via the mechanisms of solid-state transformation or replacement
364 alteration or dissolution-reprecipitation (e.g. Xia et al. 2009, 2010; Chen et al. 2010, 2011; Sheng et
365 al. 2011). In this study, only those zircons in HP/UHP metaigneous rocks from the Qinling-Tongbai-
366 Dabie-Sulu orogenic belt that give ages between 800 Ma and 600 Ma, equal to or close to the
367 Neoproterozoic protolith age, are regarded as being "igneous" in origin and most likely they have
368 preserved igneous protolith or parental magma oxygen isotope signatures. Given that three outliers
369 (samples #2, #13 & #21) are excluded, "igneous" zircons of this age occur in both HP/UHP
370 metaigneous rocks and Neoproterozoic granites that have Th/U ratio $\geq$ ca. 0.3 and $\delta^{18}O$ value $\geq$ –
371 1.7‰ (Fig. 6b). In contrast, most zircons with ages between 245 Ma and 200 Ma, including those
372 from syn-orogenic pegmatites (#10, #14 & #15; Wallis et al. 2005), have Th/U ratio $\leq$ ca. 0.3 and
373 highly variable $\delta^{18}O$ value ranging between –8.5‰ and 9.1‰ (Fig. 6c). In other words, there appears
374 to be no difference in Th/U between Triassic pegmatite/granitic leucosome zircons and other
375 contemporaneous HP/UHP metamorphic zircons (see also Liu et al. 2010b, 2012), in contrast to
376 igneous zircons from other syn-orogenic intrusions, where the values are mostly $\geq$ 0.5 (e.g. Zhao et al.
377 2012). Metamorphic zircon is used here to describe those zircons (or zircon rims) *newly formed* from

aqueous fluids or hydrous melts or where *complete recrystallization of* protolith zircons has occurred during Triassic metamorphism, including three different stages — prograde, peak HP/UHP, and retrograde metamorphic stages — as demonstrated especially for UHP marbles and marble-hosted UHP eclogites at Dabie-Sulu (e.g. Liu et al. 2006a,b; Wu et al. 2006). Nine data points (Fig. 6c) for 7 zircons with Th/U ratios > ca. 0.3, from both eclogites (#32, #47 & #61) and orthogneisses (#3 & #25), are also omitted from further discussion. It should be pointed out that the contrasting Th/U ratios between Neoproterozoic "igneous" zircons and Triassic metamorphic zircons in this study are consistent with the results obtained using the same techniques (SIMS & LA-ICP-MS) for HP/UHP rocks, as well as Neoproterozoic granites in the region, that were compiled from the literature but not presented here.

Here we can assess $\delta^{18}O$ variability within a single grain in detail, for those zircons analyzed multiple times and for which age constraints are available. The intragrain $\delta^{18}O$ variability can be evaluated by using the following parameters: range in $\delta^{18}O$ within "igneous" or metamorphic zircon (or domain) and $\Delta^{18}O$ (M-Zrn – I-Zrn) for the variation in $\delta^{18}O$ between "igneous" zicons and metamorphic zircons from individual rock samples.

Metamorphic zircons in one retrograded eclogite sample (#66) have a narrow range in $\delta^{18}O$, between 3.2‰ and 4.2‰ (n=18), with an identical average value (3.8‰) for two age groups (223 Ma versus 208 Ma; Liu et al. 2010a). This suggests that there is little or no oxygen isotopic shift in the rock system from the peak metamorphic stage to the retrograde stage. Metamorphic zircons in two other samples (#33 & #39) are also relatively homogeneous in $^{18}O/^{16}O$ and they have an average $\delta^{18}O$ value of –3.3±0.5‰ (n=10) and 2.4±0.7‰ (n=14), respectively (ESM S1).

Available average $\delta^{18}O$ values for metamorphic zircons with ages between 245 Ma and 200 Ma from other Tongbai-Dabie-Sulu rocks range from –8.3‰ to 6.8‰ (ESM S1). Only one pegmatite (#10) and four orthogneisses (#8, #11, #24 & #54) give a 2 SD value of ±2.0‰ to ±6.1‰ from the average calculation, indicating pronounced intergrain variability in $\delta^{18}O$.

The criteria for evaluation of oxygen isotopic equilibrium at *inter-* or *intra-crystalline scale* varies according to the analytical method used in different studies. There are no available ion

405 microprobe $\delta^{18}O$(Grt) data for the Tongbai-Dabie-Sulu HP/UHP rocks, although certain intragrain
406 $\delta^{18}O$-variations in garnets from eclogites and granulite-facies metamorphic rocks elsewhere have been
407 reported (Vielzeuf et al. 2005; Page et al. 2010; Russell et al. 2012). We can only utilize the laser
408 fluorination results (ca. 300 μm spot size), which are indicative of gradients of $\delta^{18}O$ within garnets
409 (ca. 1 cm in diameter) of no more than 1‰ (Xiao et al. 2001, 2002). Thus, we can use a $\delta^{18}O$(M-Zrn)
410 *versus* $\delta^{18}O$(Grt) diagram to evaluate the oxygen isotopic equilibrium between metamorphic zircon
411 and garnet only on a hand specimen scale by comparison between the average $\delta^{18}O$ values for
412 metamorphic zircons ($n \geq 4$, 2 SD $\leq \pm 0.8$‰; SIMS) and the bulk data for garnets (laser fluorination).
413 The equilibrium oxygen isotope fractionation between zircon and garnet is less than 0.2‰ at high
414 temperatures (>600ºC; Zheng et al. 1993a; Valley et al. 2003) and if these minerals equilibrated
415 during peak HP/UHP metamorphism, their oxygen isotope ratios should be nearly identical. All data
416 points for 5 of the studied samples fall along the $\Delta = 0$ line in Fig. 3 and the $\Delta^{18}O$(M-Zrn – Grt) values
417 range between –0.2 and 0.2‰, within the analytical precision. These small $\Delta^{18}O$(M-Zrn – Grt) values
418 for a very limited number of samples suggest that approximate oxygen isotopic equilibrium between
419 metamorphic zircon, like other eclogitic minerals, and garnet is attained and preserved during peak-
420 HP/UHP metamorphism in these samples at the hand specimen scale, and that the average $\delta^{18}O$ values
421 for metamorphic zircons, $\delta^{18}O$(M-Zrn), can be used to approximately estimate bulk composition of
422 the host rock during metamorphism.

423 $\delta^{18}O$ for a few Neoproterozoic "igneous" zircon grains (or cores) varies by 2.6-7.7‰ (e.g.
424 Figs. 2a & 2b). About one-third of Neoproterozoic "igneous" zircons, mostly from eclogites and
425 orthogneisses, have a $\delta^{18}O$ value below 4‰ and down to –1.7‰ (Fig. 6b). The lowest $\delta^{18}O$ (<0)
426 values are from a Cretaceous leucosome (#53) in dioritic orthogneiss enclosed in gneissic granite at
427 Xinzhuang from the Tongbai Complex (Figs. 2d & 7c). This is the first ion microprobe report of such
428 low-$\delta^{18}O$ igneous zircon cores of Neoproterozoic ages in rocks from Tongbai. Data for individual
429 rock samples from other localities such as Qinglongshan–Hushan (Sulu; #1-4), Shuanghe (Dabie; #20
430 & #21) and Sidaohe (Hong'an; #37-39) are also shown in Figs. 7a & 7b for comparison. In a given

sample, $\delta^{18}O$ for Neoproterozoic "igneous" zircon is commonly equal to or higher than that for Triassic metamorphic zircons or even Cretaceous igneous zircons.

Average $\delta^{18}O$ values for Neoproterozoic "igneous" zircons (800-600 Ma) in samples from the Tongbai-Dabie-Sulu orogenic belt vary from –0.9‰ to 6.9‰; 2 SD is mostly ≤ ±2.1‰ (ESM S1), some of which are lower than the value (5.3±0.6‰) of zircon in equilibrium with a mantle-derived magma (Valley et al. 2005). Neoproterozoic "igneous" zircons in sample #62 have a narrow range in $\delta^{18}O$, varying by only 0.6‰ (average = 4.7±0.3‰, n=10). Pronounced intergrain variability in $\delta^{18}O$ for Neoproterozoic "igneous" zircons is observed in 2 other samples (#2 & #26), as indicated by 2 SD up to ±3.6‰ (ESM S1). To some extent, the more variable $\delta^{18}O$ values preserved in Neoproterozoic "igneous" than that of metamorphic zircons may be explained by either zircon inheritance or parental magma heterogeneity, if post-magmatic modifications that may be pronounced for zircons with ages between 600 and 245 Ma (Figs. 6a & 7) are precluded.

$\Delta^{18}O$ (Metamorphic Zircon – Igneous Zircon): Grouping the Host Rocks

A plot of $\delta^{18}O$ for "igneous" zircons *versus* $\delta^{18}O$ for metamorphic zircons can be used to show which rocks that have been infiltrated by externally derived fluids. Figure 8a plots $\delta^{18}O$ for Triassic metamorphic zircon rims (245-200 Ma) *versus* Neoproterozoic "igneous" zircon cores (800-600 Ma), but only for some of the investigated samples due to limited data that allow correlation of age with $\delta^{18}O$ values. In addition, $\delta^{18}O$ for zircons in a pegmatite (#15), metamorphic zircons without age constraints (2 SD ≤ ±1.2‰, for average $\delta^{18}O$; ESM S1) from a UHP eclogite (#2) and two granitic orthogneisses (#4 & #20; Fig. 4) are also included in this diagram to enlarge the dataset. Here, a negligible deviation of average $\delta^{18}O$ of –6.4±0.7‰ (n=17) for metamorphic zircons in one of the samples (#20) from that for epidote, (–6.5‰ in Fu et al. 1999), confirms approximate oxygen isotopic equilibrium between the two minerals at high temperatures (Zheng 1993a,b).

Overall, Neoproterozoic "igneous" zircons from eclogites and orthogneisses commonly have equal or higher average $\delta^{18}O$ values than Triassic metamorphic zircons in the same samples. The data for metaigneous rocks can be split into four groups (I to IV) in Fig. 8a. Rocks of Group I have both

Neoproterozoic "igneous" zircons and Triassic metamorphic zircons that have similar *average* $\delta^{18}O(Zrn)$ values and approximate the mantle value of 5.3±0.6‰ (Valley 2003). This group includes one orthogneiss sample (#55; and possibly #7, see Fig. 4) and one pegmatite sample (#15). Group II has similar $\delta^{18}O$(I-Zrn) to Group 1, but significantly lower $\delta^{18}O$(M-Zrn or garnet): $\delta^{18}O$(M-Zrn) = –4.5‰ to 2.3‰, and $\delta^{18}O$(I-Zrn) = 4.7‰ to 5.2‰. Three orthogneiss samples (#8, #13, #54) make up this grouping. Group III contains only one granitic orthogneiss sample (#4) that has low-$\delta^{18}O$ zircons that are equilibrated, $\delta^{18}O$(M-Zrn) ≈ $\delta^{18}O$(I-Zrn) < 4.0‰. Rocks of Group IV are characterized by much lower $\delta^{18}O$ values in Triassic metamorphic zircons than in Neoproterozoic "igneous" zircons (below 4‰), i.e. $\Delta^{18}O$(M-Zrn – I-Zrn) = –11.6‰ to –4.3‰ and $\delta^{18}O$(M-Zrn) = –9.9‰ to –4.5‰. The rocks of Group IV are one UHP eclogite (#2) and four granitic orthogneisses (#3, #5, #20 & #21). Here, exceptionally high $\delta^{18}O$ values (6.3‰ to 9.5‰; Fig. 4) for one inherited zircon grain (no. 15) from the eclogite were omitted from the calculation.

As discussed above, $\delta^{18}O$ values of Triassic metamorphic zircon are approximately equilibrated with metamorphic garnet $\delta^{18}O$ values (Fig. 3), whereas $\delta^{18}O$ of Neoproterozoic "igneous" zircon cores record the $\delta^{18}O$ values of the original pre-metamorphic magmatic rocks. The $\delta^{18}O$ values of these latter zircons may also reflect the whole-rock $\delta^{18}O$ value at the time of crystallization, i.e. during magmatism or earlier metamorphism (see Valley 2003; Page et al. 2007a). Since the oxygen isotope index (I-^{18}O) of a mineral relative to that of a reference mineral can be used to quantify the degree of ^{18}O-enrichment in the former, Zhao and Zheng (2002) were the first to demonstrate that the oxygen isotope index values increase with SiO_2 content from felsic to mafic to ultramafic rocks. For calc-alkaline plutonic rocks, the empirical oxygen isotopic fractionation between igneous zircon and the host magma, $\Delta^{18}O$(I-Zrn – WR), is approximately a linear function of SiO_2 composition (Lackey et al. 2008):

$$\Delta^{18}O(\text{I-Zrn} - \text{WR}) \approx -0.0612 \times (\text{wt.\% } SiO_2) + 2.5 \qquad \text{Equation (1).}$$

The effect of magmatic temperature on $\delta^{18}O$(I-Zrn) is relatively small (Valley 2003; Grimes et al. 2011).

Data points for two groups of metaigneous rock (Group I and Group III) fall near the $\Delta = 0$ line in Fig. 8a, suggesting approximate equilibration. Groups I and III therefore represent igneous rocks that intruded, crystallized, and were metamorphosed in a system that had no significant isotopic exchange with externally-derived fluids or country rocks with contrasting $\delta^{18}O$ after the formation of igneous zircon, i.e. at any stage between crystallization of the magma and HP/UHP metamorphism. In an igneous rock, other rock-forming minerals such as feldspar are less resistant than zircon to isotopic exchange during hydrothermal alteration (e.g. Cole and Chakraborty 2001; Valley 2003; Cole et al. 2004; Niedermeier et al. 2009) and the whole-rock $\delta^{18}O$ value decreases with hydrothermal alteration.

Data points for the two other groups of metaigneous rock (Groups II and IV) fall below the $\Delta = 0$ line in Fig. 8a, suggesting that minerals other than igneous zircons in the protoliths exchanged isotopes with surface waters at high temperature prior to crystallization of metamorphic zircons. Among geologically important reservoirs, only surface waters are sufficiently low in $\delta^{18}O$ (ca. 0 for seawater and down to –40‰ for glacial meltwater; Hoefs 2004) to affect this exchange. The oxygen isotope fractionation between a mineral and water gets much smaller at higher temperatures, e.g. < ±1.5‰ at T > 700ºC for quartz or feldspar (O'Neil and Taylor 1967; Clayton et al. 1972; Zheng 1993a). The oxygen isotopic equilibrium between metamorphic zircon and garnet for many rocks argues against such fluid infiltration and/or significant diffusion under post-HP/UHP metamorphic conditions. Any post-UHP fluid-rock interactions would cause retrogression of the eclogitic rocks into amphibolite and/or greenschist facies mineral assemblages and thus lead to retrograde oxygen isotope exchange during exhumation. Thus, rocks of Group II and Group IV were fluid-infiltrated after crystallization of the host magma and prior to HP/UHP metamorphism. This caused extensive hydrothermal alteration of the igneous protoliths by ancient meteoric water at high temperatures.

The low-$\delta^{18}O$ values for igneous zircon from rocks of Groups III & IV can be interpreted as resulting from remelting of hydrothermally altered wall rocks that exchanged with meteoric water at high temperatures prior to crystallization of later magma (e.g. Taylor 1986; Bindeman and Valley 2001). In other words, the mechanism to generate low-$\delta^{18}O$ magmas is through episodic intrusion and

510 interaction with heated surface water where younger plutons melt previously altered, low-$\delta^{18}O$ wall
511 rocks.

512 $\delta^{18}O$(Zrn) for other rocks, such as felsic granulite and metasedimentary rocks, is not shown in
513 Fig. 8a due to poor age constraints. However, we recall results presented elsewhere in the literature
514 where it was noted that higher-$\delta^{18}O$ values for metamorphic than for igneous or detrital zircons
515 [$\Delta^{18}O$(M-Zrn – I-Zrn), up to 7.1‰] are observed in Naxos, Greece (Martin et al. 2008) and the
516 Adirondack Mountains, New York (Page et al. 2007a; Lancaster et al. 2009). The significant increase
517 in $\delta^{18}O$ from igneous core to metamorphic rim can be interpreted as resulting from metamorphic
518 growth of zircon in oxygen isotopic equilibrium with contemporaneous high-$\delta^{18}O$ minerals in the host
519 metasedimentary rocks via subsolidus reactions rather than by volume diffusion at high temperatures.
520 This is in contrast to the results for zircons in metaigneous rocks at Tongbai-Dabie-Sulu, which
521 commonly have negative $\Delta^{18}O$(M-Zrn – I-Zrn) values, suggesting post-magmatic, hydrothermal
522 alteration of the igneous protoliths.
523

524 **Genesis of Neoproterozoic Low-$\delta^{18}O$ Magmas: Comparison with Yellowstone Caldera**

525 Worldwide, few low-$\delta^{18}O$ igneous zircons, i.e. igneous zircons with $\delta^{18}O$ values below 4‰,
526 have been reported. Where present, pristine low-$\delta^{18}O$ igneous rocks (or magmas) from young terranes
527 that have $\delta^{18}O$ whole-rock values lower than primitive magma compositions or the mantle (5.3±0.6‰;
528 Valley 2003) have been intensively studied, especially in shallow subvolcanic environments such as
529 Heise, Yellowstone, Iceland and the British Hebrides (e.g. Bindeman and Valley 2001; Monani and
530 Valley 2001; Valley et al. 2005; Thirlwall et al. 2006; Bindeman et al. 2008a,b; Watts et al. 2011,
531 2012).

532 The presence of low-$\delta^{18}O$ igneous zircons in eclogite and granitic orthogneiss (Groups III &
533 IV, Fig. 8a) requires a complex history to explain the pre-UHP ^{18}O-depletion. For comparison with
534 Yellowstone caldera, we will use a two-stage ^{18}O-depletion model proposed by Fu et al. (2006) to
535 illustrate the ^{18}O-depletion processes. In a similar model proposed by Zheng et al. (2007a, 2008), two
536 episodes of rift magmatism were invoked (at ca. 780 and ca. 760-750 Ma) throughout the Dabie and

537 Sulu terranes rather than requiring repeated sub-caldera magmatism at individul places to cause the
538 extreme ^{18}O-depletion.

539 The processes proposed for Tongbai-Dabie-Sulu are essentially similar to those documented
540 by analysis of $\delta^{18}O$ in zircons and quartz from rhyolites at Yellowstone Caldera (Bindeman and
541 Valley 2001, Bindeman et al. 2008a). The oxygen isotope fractionation between quartz and zircon
542 yields the empirically or experimentally expected values for equilibrium at magmatic temperatures
543 [$\Delta^{18}O(Qz\text{-}Zrn)$ = 2.5-1.8‰ at 750-850ºC; Valley et al. 2003; Trail et al. 2009] in high (normal)
544 $\delta^{18}O(Qz)$ (4.1‰ to 7.9‰) pre-caldera and extra-caldera lavas and tuffs at Yellowstone [average
545 $\Delta^{18}O(Qz\text{-}Zrn) = 2.3\pm0.4$‰, n=21; Bindeman and Valley 2001]. It is noted that the $\Delta^{18}O(Qz\text{-}Zrn)$
546 values are lower than that estimated using the theoretical calibration of Zheng (1993a): 4.0-3.6‰ at
547 750-850ºC. In contrast, low-$\delta^{18}O$ lavas [$\delta^{18}O(Qz) \leq 2.7$‰] are characterized by low or reversed
548 $\Delta^{18}O(Qz\text{-}Zrn)$ values (down to –0.5‰; Bindeman and Valley 2001), which indicate isotopic
549 disequilibrium. In other words, the low-$\delta^{18}O$ quartz phenocrysts have a lower $\delta^{18}O$ value than
550 expected for equilibrium with zircon at high temperatures. This is interpreted to result from
551 hydrothermal alteration of earlier crystallized magmas, which were remelted to form low-$\delta^{18}O$ lavas.
552 However, zircons within these lavas include cores that were never altered and that preserve original
553 higher $\delta^{18}O$ values and were cannibalized or recycled from the wall-rocks ("cannibalism": Bindeman
554 and Valley 2001; Monani and Valley 2001).

555 Average $\delta^{18}O$ values for in situ analyses of igneous zircon cores are plotted *versus* igneous
556 zircon rims in Fig. 8b (Table 2 of Bindeman et al. 2008a), for individual volcanic rock samples from
557 Yellowstone. Three broad groups of rocks (A, B, C) can be identified to illustrate the sub-caldera
558 model. Group A includes two samples dated at 2.04 Ma that have mantle-like oxygen isotope ratios
559 for igneous zircons (core and rim). Group B includes 5 samples that have an age between 1.78 and
560 0.11 Ma and where $\delta^{18}O(I\text{-}Zrn\ rim) \approx \delta^{18}O(I\text{-}Zrn\ core) \leq 4$‰. Group C includes 3 samples with an
561 age of approximately 0.5 Ma, where $\delta^{18}O(I\text{-}Zrn\ rim) << \delta^{18}O(I\text{-}Zrn\ core) \leq 4$‰. Magmatism at
562 Yellowstone started with the Group A, i.e. 2.04 Ma. Low-$\delta^{18}O$ magmas formed at several stages. Note
563 that an outlier (2.0 Ma) has an average $\delta^{18}O(I\text{-}Zrn\ rim)$ higher than that of the igneous zircon cores.

The zircons in both the Tongbai-Dabie-Sulu metaigneous rocks (eclogite and granitic orthogneiss) and the Yellowstone rhyolites (Bindeman et al. 2008a) display core-rim structures as revealed by CL imaging; and the igneous zircon (or domain) $\delta^{18}O$ in both areas can be below 0, and even down to ca. –2‰. However, one pronounced difference between the two areas is that zircon rims at Yellowstone are igneous, whereas zircon rims at Tongbai-Dabie-Sulu are metamorphic. Also, the volcanic rocks at Yellowstone have never been deeply buried and, based on Eqn. 1, the average $\delta^{18}O$ zircon rim represents the oxygen isotope composition of magma after assimilation or melting of hydrothermally altered rocks. If such low-$\delta^{18}O$ igneous rocks were metamorphosed at high temperatures, newly formed metamorphic zircon could crystallize and would be in equilibrium with other low-$\delta^{18}O$ metamorphic minerals such as garnet or quartz (cf. Chen et al. 2011). Such low-$\delta^{18}O$ metaigneous rocks would thus be similar to the rocks of Groups II and IV at Tongbai-Dabie-Sulu (Fig. 8a).

Spatial Distribution of Neoproterozoic Low-$\delta^{18}O$ Magmas in the South China Block

Neoproterozoic low-$\delta^{18}O$ (meta-) igneous rocks are widespread in the Tongbai-Dabie-Sulu orogenic belt. In addition to this study, a Neoproterozoic metagranite from Zaobuzhen (ZBZ in Fig. 1a) in the easternmost part of the Sulu terrane gives an $\delta^{18}O$ zircon value varying from –7.8‰ to –3.1‰ (bulk analysis) along a profile of 50 m length (Tang et al. 2008a). At Huangzhen in the South Dabie low-T/UHP eclogite-facies unit (HZ in Fig. 1b), low-T/high-P eclogites and associated granitic orthogneisses have $\delta^{18}O$ values as low as –4.3‰ for zircon and –6.3‰ for garnet (bulk analysis; e.g. Zheng et al. 1999; Li et al. 2004; Xia et al. 2008). A Neoproterozoic granite from Luzhenguan in North Dabie (LZG in Fig. 1b) that extends to the Beihuaiyang low-T/low-P greenschist-facies zone, has a $\delta^{18}O$(Zrn) value of 0.6‰ (bulk analysis; Zheng et al. 2004), even lower than the Danlongsi granite (#26). Low-$\delta^{18}O$ UHP rocks at Sulu also occur down to depths of ca. 3 km from the surface, as determined from the CCSD-MH drill cores (e.g. Xiao et al. 2006; Chen et al. 2007). Although the presence of Neoproteoroizc low-$\delta^{18}O$ igneous zircons in these rocks is yet to be confirmed by SIMS analysis, it appears that low-$\delta^{18}O$ magmas of Neoroterozoic age are not restricted to UHP units at

Dabie-Sulu or in the Tongbai Complex. If the Neoproterozoic low-$\delta^{18}O$ (meta-) igneous rocks are centers of pre-UHP metamorphic, paleo-hydrothermal systems, this may provide a key to reconstructing specific Neoproterozoic geological environments in the region.

The Neoproterozoic metaigneous rocks at Tongbai-Dabie-Sulu represent one of the largest terranes of low-$\delta^{18}O$ magmas known on Earth. If our model is correct, their wide distribution requires a protracted series of sub-caldera events at a terrane scale because by volume the Tongbai-Dabie-Sulu orogenic belt is tens of times larger than the Yellowstone plateau (ca. 6000 km^3; Hildreth et al. 1991). The Snake River Plain, composed dominantly of felsic lavas, is the only known low-$\delta^{18}O$ magmatic terrane of comparable size. Given that the Dabie and Sulu terranes were joined prior to displacement of ca. 530 km along the sinistral Tancheng-Lujiang Fault (e.g. Okay and Sengör 1992), the distribution pattern of low-$\delta^{18}O$ rocks in the South China Block is considered to be linear. Thus the linear trend and dimensions of low-$\delta^{18}O$ rocks at Tongbai-Dabie-Sulu are similar to the bimodal basaltic and silicic volcanism of the Neogene Snake River Plain – Yellowstone Plateau volcanic province, which is >600 km long (e.g. Savov et al. 2009). The latter represents a single magmatic system (developed over 17 myr) that has been interpreted to result from an eastward migrating Yellowstone hotspot relative to the North American plate (e.g. Leeman et al. 2008). It is noted that extensive crustal processes such as remelting of pre-existing low-$\delta^{18}O$ crust, e.g. meteoric-hydrothermal altered granitic rocks of the Idaho batholith, may also precede generation of the earliest rhyolite magmas especially in the central Snake River Plain (e.g. Boroughs et al. 2005, 2012; Leeman et al. 2008). The Isle of Skye within the British Tertiary Igneous Province is also regarded as recording a hotspot track (e.g. Stuart et al. 2000) and represents a comparably large low-$\delta^{18}O$ magmatic terrane (e.g. Monani and Valley 2001). We therefore propose that the Tongbai-Dabie-Sulu Neoproterozoic low-$\delta^{18}O$ igneous province may be related to a migrating hotspot relative to the South China Block during the Neoproterozoic. One may argue that there are no systematic age variations in the Neoproterozoic low-$\delta^{18}O$ igneous protoliths at Tongbai-Dabie-Sulu to support this hypothesis (ESM S1; see also Zheng et al. 2003, 2008, 2009). However, this would require further improved high-precision, high-accuracy geochronological research on zircons, especially from pristine

Neoproterozoic granitoids in order to resolve any small age differences, e.g. by U-Pb chemical abrasion TIMS analysis (Mattinson 2005; Davydov et al. 2010). This would also help to better constrain the timing of Neoproterozoic magmatism in the region, and whether it was continuous or episodic.

Zircons with slightly low-$\delta^{18}O$ values are also present in both rhyolite and granite of the Baoxing Complex (#73 & #77; Figs. 2e & 2f). This is also the first by SIMS reported in the western margin of the South China Block, where other Neoproterozic igneous rocks, such as in the Pengguan, Xuelongbao and Kangding complexes, are widespread (e.g. Zhou et al. 2002, 2006; Yan et al. 2008; Fig. 1d). Bulk analysis indicates that rocks from the Kangding Complex have mantle-like $\delta^{18}O$(Zrn) values of 4.2-6.2‰ (Zheng et al. 2007b) and that many samples from the Huangling Granitoid have $\delta^{18}O$(Zrn) values varying from 4.9 to 6.8‰ (Zhang et al. 2008, 2009). This is in contrast to the relatively high $\delta^{18}O$(Zrn) values (≥ ca. 7‰) for Neoproterozoic rocks from some other parts of the South China Block (Zheng et al. 2007b). Zhou et al. (2006) argue that, together with the arc signatures of other granites and mafic intrusions in the region, the 750 Ma Xuelongbao Adakitic Complex was likely derived from partial melting of a subducted oceanic slab. The Neoproterozoic mafic intrusions and granitoids of the Hannan and Micangshan massifs from the northwestern margin of the South China Block (i.e. South Qinling) are also interpretd to be subduction-related (e.g. Dong et al. 2011, 2012). In this regard, it appears that the western margin of the South China Block had a prolonged history of magmatism during the Neoproterozoic and that, like the present-day northern margin of the South China Block (i.e. the Tongbai-Dabie-Sulu orogenic belt), the slightly low-$\delta^{18}O$ zircons may also be attributed to extensive high-temperature hydrothermal alteration subsequent to either subduction-related or rift-related magmatism. However, so far no negative $\delta^{18}O$ zircons have been identified from rocks along the western margin of the South China Block, suggesting that the slightly low $\delta^{18}O$ values in this region more likely resulted from the involvement of high-temperature seawater in the hydrothermal alteration. This is the subject of ongoing investigations.

Wang et al. (2011a) reported that most low-$\delta^{18}O$ igneous zircons of detrital origin, extracted from four Cryogenian sedimentary rocks in the Nanhua Rift basin, have ages of 800-700 Ma and that low-$\delta^{18}O$ igneous zircons started to appear from ca. 870 Ma, coinciding with the onset of extension

and continental rifting. These authors argue that the occurrence of a sharp oxygen isotope shift from the highest $\delta^{18}O$ value of 12.2‰ (ca. 820 Ma) to the lowest of 2.0‰ (ca. 780 Ma) is contemporaneous with the onset of large-scale lithopheric extension and plume activities in the South China Block. Zircons with the lowest-$\delta^{18}O$ (<4‰) values are further interpreted to have formed from remelting of 825-810 Ma igneous rocks related to the continental flood basalt event that isotopically exchanged with surface water at high temperatures (Wang et al. 2012). When taken together, it is evident that many Neoproterozoic low-$\delta^{18}O$ igneous rocks in the South China Block indeed predate the well-documented Neoproterozoic glacial events (Zheng et al. 2007a, 2008; Wang et al. 2011a; this study). However, the potential involvement of recycled meltwaters from possible local continental glaciations, rather than the well-documented global Neoproterozoic glaciations, cannot completely be ruled out.

GEOLOGICAL IMPLICATIONS

The $\delta^{18}O$ values for zircons formed during other magmatic and metamorphic events in the region and their geological significance are discussed here. The U-Pb ages of detrital zircons from quartzites (#23 & #63), paragneisses (#9, #28, #58 & #60) and pelitic schist (#50), as well as marble and felsic granulite from the Tongbai-Dabie-Sulu orogenic belts, support the conclusion that widespread Archean to Paleoproterozoic tectonothermal events took place at the northern margin of the South China Block (e.g. Ayers et al. 2002; Chen et al. 2003; Liu et al. 2006a, 2008, 2010a; Wu et al. 2006, 2008b; Sun et al. 2008; Jian et al., 2012; this study). In addition, many Paleoproterozoic metamorphic zircons (2.1-1.7 Ga) from paragneiss (#60) and pelitic schist (#50; see Figs. 2g & 2h) have relatively high $\delta^{18}O$ values of ca. 10‰ and ca. 13‰, respectively. In contrast, $\delta^{18}O$ for many other zircons of the same age, and the majority of Archean to early Paleoproterozoic zircons (>2.1 Ga) from other metasedimentary rocks, range from mantle-like values to higher than 6.5‰ (Fig. 6a). In combination with available hafnium isotope data (e.g. Wang et al. 2012), this suggests episodic growth and reworking of older continental crust in the South China Block throughout geological time.

It appears that a consensus on the presence of recycled pre-collision oceanic crust in the Hong'an terrane has recently been reached (e.g. Wu et al. 2009; Liu et al. 2011 and references therein). In a HP eclogite (sample #30), metamorphic zircons with ages of 305 Ma have an $\delta^{18}O$ value of 9.5±0.8‰ (n=5), whereas $\delta^{18}O$ for two zircon grains (or domains) interpreted to be igneous, with ages of ca. 380 Ma, is as high as 10.5‰ (Figs. 2i & 2j). Other eclogite samples also from Xiongdian have positive $\varepsilon_{Nd}(t)$ values (e.g. Jahn et al. 2005), distinct from the highly negative values of most of the Dabie-Sulu HP/UHP eclogites (e.g. Jahn et al. 1999 and references therein), and high $\delta^{18}O$(Grt) values (8.1-11.4‰; Fu et al. 2002; Jahn et al. 2005). The $^{206}Pb/^{238}U$ zircon age for the Xiongdian HP eclogites varies from 424 Ma to ca. 300 Ma (e.g. Jian et al. 2000; Gao et al. 2002; Sun et al. 2002; Cheng et al. 2009; Peters et al. 2012; this study). Moreover, zircons have initial epsilon Hf values [$\varepsilon_{Hf}(t)$] of –11 to +18 (Peters et al. 2012). Thus, the Xiongdian eclogites could represent Middle Silurian – Early Devonian mafic volcanic rocks that record a different tectonic history from other HP/UHP metamorphic rocks in the Tongbai-Dabie-Sulu orogenic belt, although the presence of Proterozoic crustal components cannot be precluded. In this regard, the protolith likely formed part of ancient oceanic crust that may have experienced low-temperature seafloor alteration prior to Carboniferous HP metamorphism. While some of the altered basaltic rocks from mid-ocean ridges have whole-rock $\delta^{18}O$ value as high as 10‰ (Gregory and Taylor 1981; Eiler 2001), zircons appear to preserve the mantle-like $\delta^{18}O$ value (5.2-5.3‰; Cavosie et al. 2009; Grimes et al. 2011) and are resistant to seafloor hydrothermal alteration and/or low-T/HP metamorphism (Fu et al. 2012). In this scenario, newly crystallized metamorphic zircons from high-$\delta^{18}O$ altered rocks could have such high $\delta^{18}O$ values.

The average $\delta^{18}O$(Zrn) values of ca. 4.1‰ to 5.6‰ for post-orogneic intrusions or pegmatites at Tongbai (ESM S1) are consistent with the results of previous studies: 3.9‰ to 7.7‰, for Cretaceous mafic-ultramafic rocks from Dabie (Xia et al. 2002; Zhao et al. 2005) and 3.2‰ and 6.4‰ for Cretaceous granites and diorites, respectively, from Sulu (Huang et al. 2006). The incorporation of Neoproterozoic zircons, together with the lower $\delta^{18}O$ zircons in Cretaceous igneous rocks than primitive magma compositions, suggest that recycled Neoproterozoic hydrothermally altered

699 supracrustal materials may be involved in post-orogenic magmatism in the area (e.g. Zhao et al. 2004,
700 2007; Huang et al. 2006; Xie et al. 2006; Dai et al. 2011).
701
702 **CONCLUSIONS**
703 Zircons in granite, pegmatite, metagabbro, eclogite, garnet amphibolite, granitic and dioritic
704 orthogneiss, paragneiss, schist, quartzite and felsic granulite from the Tongbai-Dabie-Sulu orogenic
705 belt, east-central China, have been analyzed in situ for oxygen isotope ratio and age. Average $\delta^{18}O$
706 values for Triassic metamorphic zircons in the samples range from –9.9‰ to 6.8‰, whereas average
707 $\delta^{18}O$ values for Neoproterozoic "igneous" zircon (800-600 Ma) vary from –0.9‰ to 6.9‰. Average
708 $\Delta^{18}O$ values between metamorphic and "igneous" zircons vary from –11.6‰ to 0.9‰. The lowest
709 $\delta^{18}O$ (down to ca. –2.0‰) Neoproterozoic "igneous" zircons are from Cretaceous leucosome in
710 dioritic orthogneiss enclosed in gneissic granite at Xinzhuang, Tongbai; this is the first ion
711 microprobe report of such low-$\delta^{18}O$ Neoproterozoic igneous zircons in the region.
712 A two-stage ^{18}O-depletion model is used to explain the formation of low-$\delta^{18}O$ magmas in the
713 Tongbai-Dabie-Sulu orogenic belt, by analogy with the Yellowstone Plateau and the Isle of Skye,
714 involving repeated sub-caldera magmatic intrusion, exchange with heated meteoric water, and
715 subsequent melting of altered wall rock. The widespread occurrence of Neoproterozic low-$\delta^{18}O$
716 igneous protoliths at Tongbai-Dabie-Sulu and the comparable size (> 600 km in length) to the
717 Neogene Snake River Plain – Yellowstone Plateau volcanic province support the hypothesis that
718 Neoproterozoic bimodal magmatism at Tongbai-Dabie-Sulu took place during continental rifting of
719 the South China Block and may have been controlled by a migrating hotspot, similar to that at
720 Yellowstone, relative to the continental crust.
721
722 **Acknowledgements** — D.G. Chen, Z.H. Hou, S.B. Hu, B.P. Kohn, Y.T. Tian, S. Wallis and Y.-F.
723 Zheng provided many of the zircon separates or grain mounts. This work was supported initially by
724 the U.S. National Science Foundation (EAR-0509639) and U.S. Department of Energy (93ER14389)
725 and later by the University of Melbourne (ECR-600838). The WiscSIMS Laboratory is partly

726 supported by NSF (EAR-0319230, EAR-0516725, EAR-0744079). BF gratefully acknowledges
727 technical assistance of the AMMRF Flagship Ion Probe Facility (CMCA) at the University of Western
728 Australia, funded by the University, State and Commonwealth Governments. Earlier versions of this
729 manuscript have benefited greatly from thorough reviews by J.W. Valley, Y.-F. Zheng and several
730 anonymous referees.

731

732 **REFERENCES**

733 Ayers JC, Dunkle S, Gao S, Miller CF (2002) Constraints on timing of peak and retrograde metamorphism in
734 the Dabie Shan Ultrahigh-Pressure Metamorphic Belt, east-central China, using U-Th-Pb dating of zircon
735 and monazite. Chem Geol 186: 315-331.
736 Baker J, Matthews A, Mattey D, Rowley D, Xue F (1997) Fluid-rock interactions during ultra-high pressure
737 metamorphism, Dabie Shan, China. Geochim Cosmochim Acta 61: 1685-1696.
738 BGMRSP (Bureau of Geology and Mineral Resources of Sichuan Province) (1991) Regional Geology of
739 Sichuan Province, People's Republic of China Ministry of Geology and Mineral Resources, Beijing.
740 Geological Memoirs, Series 1, no 23, pp 1-730 (in Chinese with English abstract).
741 Bindeman I (2011) When do we need pan-global freeze to explain ^{18}O-depleted zircons and rocks? Geology 39:
742 799-800.
743 Bindeman IN, Valley JW (2001) Low-δ^{18}O rhyolites from Yellowstone: magmatic evolution based on analyses
744 of zircons and individual phenocrysts. J Petrol 42: 1491-1517.
745 Bindeman IN, Fu B, Kita NT, Valley JW (2008a) Origin and evolution of silicic magmatism at Yellowstone
746 based on ion microprobe analysis of isotopically zoned zircons. J Petrol 49: 163-193.
747 Bindeman I, Gurenko A, Sigmarsson O, Chaussidon M (2008b) Oxygen isotope heterogeneity and disequilibria
748 of olivine crystals in large volume Holocene basalts from Iceland: evidence for magmatic digestion and
749 erosion of Pleistocene hyaloclastites. Geochim Cosmochim Acta 72: 4397-4420.
750 Black LP, Kamo SL, Allen CM, Davis DW, Aleinikoff JN, Valley JW, Mundil R, Campbell IH, Korsch RJ,
751 Williams IS, Foudoulis C (2004) Improved ^{206}Pb/^{238}U microprobe geochronology by monitoring of a
752 trace-element-related matrix effect: SHRIMP, ID-TIMS, ELA-ICP-MS and oxygen isotope
753 documentation for a series of zircon standards. Chem Geol 205: 115-140.
754 Boroughs S, Wolff J, Bonnichsen B, Godchaux M, Larson P (2005) Large-vaolume, low-δ^{18}O rhyolites of the
755 central Snake River Plain, Idaho, USA. Geology 33: 821-824.
756 Boroughs S, Wolff JA, Ellis BS, Bonnichsen B, Larson P (2012) Evaluation of models for the origin of Miocene
757 low-δ^{18}O rhyolites of the Yellowstone/Columbia River Large Igneous Province. Earth Planet Sci Lett
758 313-314: 45-55.
759 Bowman JR, Moser DE, Valley JW, Wooden JL, Kita NT and Mazdab FK (2011) Zircon U-Pb isotope, δ^{18}O
760 and trace element response to 80 m.y. of high temperature metamorphism in the lower crust: sluggish
761 diffusion and new records of Archean craton formation. Am J Sci 311: 719-772.
762 Burchfiel BC, Chen ZL, Liu YP, Royden LH (1995) Tectonics of the Longmen Shan and adjacent regions,
763 central China. Int Geol Rev 37: 661-735.
764 Cavosie AJ, Kita NT, Valley JW (2009) Magmatic zircons from the Mid-Atlantic Ridge: primitive oxygen
765 isotope signature. Am Mineral 94: 926-934.
766 Cavosie AJ, Valley JW, Wilde SA, EIMF (2005) Magmatic δ^{18}O in 4400-3900 Ma detrital zircons: a record of
767 the alteration and recycling of crust in the Early Archean. Earth Planet Sci Lett 235: 663-681.
768 Chen DG, Deloule E, Cheng H, Xia QK, Wu YB (2003) Preliminary study of microscale zircon oxygen isotopes
769 for Dabie-Sulu metamorphic rocks: ion probe in situ analyses. Chinese Sci Bull 48: 1670-1678.
770 Chen DG, Deloule E, Ni T (2006) Metamorphic zircon from Xindian eclogite, Dabie Terrain: U-Pb age and
771 oxygen isotope composition. Sci China (Ser D – Earth Sci) 49: 68-76.
772 Chen RX, Zheng YF, Gong B, Zhao ZF, Gao TS, Chen B, Wu YB (2007) Oxygen isotope geochemistry of
773 ultrahigh-pres sure metamorphic rocks from 200-4000 m core samples of the Chinese Continental
774 Scientific Drilling. Chem Geol 242: 51-75.
775 Chen RX, Zheng YF, Xie LW (2010) Metamorphic growth and recrystallization of zircon: distinction by
776 simultaneous in-situ analyses of trace elements, U-Th-Pb and Lu-Hf isotopes in zircons from eclogite-
777 facies rocks in the Sulu orogen. Lithos 114: 132-154.

778 Chen YX, Zheng YF, Chen RX, Zhang SB, Li QL, Dai MN, Chen L (2011) Metamorphic growth and
779 recrystallization of zircons in extremely ^{18}O-depleted rocks during eclogite-facies metamorphism:
780 evidence from U–Pb ages, trace elements, and O–Hf isotopes. Geochim Cosmochim Acta 75: 4877–
781 4898.
782 Cheng H, King RL, Nakamura E, Vervoort JD, Zheng YF, Ota T, Wu YB, Kobayashi K, Zhou ZY (2009)
783 Transitional time of oceanic to continental subduction in the Dabie orogen: constraints from U-Pb, Lu-
784 Hf, Sm-Nd and Ar-Ar multichronometric dating. Lithos 110: 327-342.
785 CIGMR (Chengdu Institute of Geology and Mineral Resources) (2004) Geological Map of Tibetan Plateau and
786 Its Vicinity. Chengdu Map Press, Chengdu (in Chinese).
787 Clayton RN, O'Neil JR, Mayeda TK (1972) Oxygen isotope exchange between quartz and water. J Geophys Res
788 77: 3057-3067.
789 Cole DR, Chakraborty S (2001) Rates and mechanisms of isotopic exchange. In Stable Isotope Geochemistry
790 (eds JW Valley, DR Cole). Mineralogical Society of America/Geochemical Society, Washington, DC.
791 Reviews in Mineralogy and Geochemistry, v 43, pp 83-223.
792 Cole DR, Larson PB, Riciputi LR, Mora CI (2004) Oxygen isotope zoning profiles in hydrothermally altered
793 feldspars: estimating the duration of water-rock interaction. Geology 32: 29-32.
794 Cui JJ, Liu XC, Dong SW, Hu JM (2012) U–Pb and ^{40}Ar/^{39}Ar geochronology of the Tongbai complex, central
795 China: implications for Cretaceous exhumation and lateral extrusion of the Tongbai–Dabie HP/UHP
796 terrane. J Asian Earth Sci 47: 155-170.
797 Dai LQ, Zhao ZF, Zheng YF, Li QL, Yang YH, Dai MN (2011) Zircon Hf-O isotope evidence for crust-mantle
798 interaction during continental deep subduction. Earth Planet Sci Lett 308: 229-244.
799 Davydov VI, Crowley JL, Schmitz MD, Poletaev VI (2010) High-precision U-Pb zircon age calibration of the
800 global Carboniferous time scale and Milankovitch band cyclicity in the Donets Basin, eastern Ukraine.
801 Geochem Geophys Geosyst 11: Q0AA04, doi: 10.1029/2009GC002736.
802 Dong YP, Liu XM, Santosh M, Zhang XN, Chen Q, Yang C, Yang Z (2011) Neoproterozoic subduction
803 tectonics of the northwestern Yangtze Block in South China: constrains from zircon U–Pb
804 geochronology and geochemistry of mafic intrusions in the Hannan Massif. Precambrian Res 189: 66-90.
805 Dong YP, Liu XM, Santosh M, Chen Q, Zhang XN, Li W, He DF, Zhang GW (2012) Neoproterozoic
806 accretionary tectonics along the northwestern margin of the Yangtze Block, China: constraints from
807 zircon U–Pb geochronology and geochemistry. Precambrian Res 196–197: 247-274.
808 Eiler JM (2001) Oxygen isotope variations of basaltic lavas and upper mantle rocks. In Stable Isotope
809 Geochemistry (eds JW Valley, DR Cole). Mineralogical Society of America/Geochemical Society,
810 Washington, DC. Reviews in Mineralogy and Geochemistry, v 43, pp 319-364.
811 Fu B, Kita NT, Valley JW (2006) Low-δ^{18}O magmas in the Dabie-Sulu UHP metamorphic terrains (China).
812 Geochim Cosmochim Acta 70 (18S): A186 (abstr).
813 Fu B, Paul B, Cliff J, Bröcker M, Bulle F (2012) O-Hf isotope constraints on the origin of zircon in high-
814 pressure mélange blocks and associated matrix rocks from Tinos and Syros, Greece. Eur J Mineral 24:
815 277-287.
816 Fu B, Zheng YF, Touret JLR (2002) Petrological, isotopic and fluid inclusion studies of eclogites from Sujiahe,
817 NW Dabie Shan (China). Chem Geol 187: 107-128.
818 Fu B, Zheng YF, Wang ZR, Xiao YL, Gong B, Li SG (1999) Oxygen and hydrogen isotope geochemistry of
819 gneisses associated with ultrahigh pressure eclogites at Shuanghe in the Dabie Mountains. Contrib
820 Mineral Petrol 134: 52-66.
821 Gao S, Qiu YM, Ling WL, McNaughton NJ, Zhang BR, Zhang G, Zhang Z, Zhong Z, Suo ST (2002) SHRIMP
822 single zircon U-Pb geochronology of eclogites from Yingshan and Xiongdian. Earth Sci 27: 558-564 (in
823 Chinese with English abstract).
824 Gregory RT, Taylor HP Jr (1981) An oxygen isotope profile in a section of Cretaceous oceanic crust, Samail
825 ophiolite, Oman: evidence for δ^{18}O buffering of the oceans by deep (>5 km) seawater-hydrothermal
826 circulation at mid-ocean ridges. J Geophys Res 86: 2737-2755.
827 Grimes CB, Ushikubo T, John BE, Valley JW (2011) Uniformly mantle-like δ^{18}O in zircons from oceanic
828 plagiogranites and gabbros. Contrib Mineral Petrol 161: 13-33.
829 Harrison TM, Schmitt AK, McCulloch MT, Lovera OM (2008) Early (≥ 4.5 Ga) formation of terrestrial crust:
830 Lu-Hf, δ^{18}O, and Ti thermometry results for Hadean zircons. Earth Planet Sci Lett 268: 476-486.
831 Hellstrom J, Paton C, Woodhead J, Hergt J (2008) Iolite: Software for Spatially Resolved LA-(QUAD and MC)
832 ICPMS analysis. Mineralogical Association of Canada Short Course series 40, pp. 343-348,
833 Mineralogical Association of Canada, Vancouver.
834 Hildreth W, Halliday AN, Christiansen RL (1991) Isotopic and chemical evidence concerning the genesis and
835 contamination of basaltic and rhyolitic magma beneath the Yellowstone Plateau volcanic field. J Petrol
836 32: 63-138.

837 Hu J, Liu XC, Qu W, Cui JJ (2012) Zircon U-Pb ages of Paleoproterozoic metabasites from the Tongbai Orogen
838 and their geological significance. Acta Geosci Sin 33: 305-315 (in Chinese with English abstract).
839 Hoefs J (2004) Stable Isotope Geochemistry. 5th Edition, 340 pp, Springer, Berlin.
840 Huang J, Zheng YF, Zhao ZF, Wu YB, Zhou HB, Liu XM (2006) Melting of subducted continent: element and
841 isotopic evidence for a genetic relationship between Neoproterozoic and Mesozoic granitoids in the Sulu
842 orogen. Chem Geol 229: 227-256.
843 Ickert RB, Hiess J, Williams IS, Holden P, Ireland TR, Lanc P, Schram N, Foster JJ, Clement SW (2008)
844 Determining high precision, in situ, oxygen isotope ratios with a SHRIMP II: analyses of MPI-DING
845 silicate-glass reference materials and zircon from contrasting granites. Chem Geol 257: 114-128.
846 Jahn BM, Liu X, Yui TF, Morin N, Bouhnik-Le Coz M (2005) High-pressure/ultrahigh-pressure eclogites from
847 the Hong'an Block, East-Central China: geochemical characterization, isotope disequilibrium and
848 geochronological controversy. Contrib Mineral Petrol 149: 499-526.
849 Jahn BM, Wu FY, Lo CH, Tsai CH (1999) Crust-mantle interaction induced by deep subduction of the
850 continental crust: geochemical and Sr-Nd isotopic evidence from post-collisional mafic-ultramafic
851 intrusions of the northern Dabie complex, central China. Chem Geol 157: 119-146.
852 Jian P, Kröner A, Zhou, GZ (2012) SHRIMP zircon U–Pb ages and REE partition for high-grade metamorphic
853 rocks in the North Dabie complex: insight into crustal evolution with respect to Triassic UHP
854 metamorphism in east-central China. Chem Geol 328: 49-69.
855 Jian P, Liu DY, Yang WR, Williams IS (2000) Petrographic and SHRIMP studies of zircons from the
856 Caledonian Xiongdian eclogite, northwestern Dabie Mountains. Acta Geol Sin 74: 766-773.
857 Jeon H, Williams IS, Chappell BW (2012) Magma to mud to magma: rapid crustal recycling by Permian granite
858 magmatism near the eastern Gondwana margin. Earth Planet Sci Lett 319-320: 104-117.
859 Kelly J, Fu B, Kita NT, Valley JW (2007) Optically continuous silcrete quartz cements of the St. Peter
860 Sandstone: high precision oxygen isotope analysis by ion microprobe. Geochim Cosmochim Acta 71:
861 3812-3832.
862 Kemp AIS, Hawkesworth CJ, Foster GL, Paterson BA, Woodhead JD, Hergt JM, Gray CM, Whitehouse MJ
863 (2007) Magmatic and crustal differentiation history of granitic rocks from Hf-O isotopes in zircon.
864 Science 315: 980-983.
865 Kita NT, Ushikubo T, Fu B, Valley JW (2009) High precision SIMS oxygen isotope analyses and the effect of
866 sample topography. Chem Geol 264: 43-57.
867 Lackey JS, Valley JW, Chen JH, Stockli DF (2008) Dynamic Magma Systems, Crustal Recycling, and
868 Alteration in the Central Sierra Nevada Batholith: the Oxygen Isotope Record. J Petrol 49: 1397-1426.
869 Lancaster PJ, Fu B, Page FZ, Kita NT, Bickford ME, Hill BM, McLelland JM, Valley JW (2009) Genesis of
870 metapelitic migmatites in the Adirondack Mts., New York. J Metamorphic Geol 27: 41-54.
871 Leeman WP, Annen C, Dufek J (2008) Snake River Plain - Yellowstone silicic volcanism: implications for
872 magma genesis and magma fluxes. In Dynamics of Crustal Magma Transfer, Storage and Differentiation
873 (eds C Annen, GF Zellmer). Geological Society, London, Special Publications, v 304, pp 235-259.
874 Li QL, Li SG, Hou ZQ, Hong J, Yang W (2005) A combined study of SHRIMP U-Pb dating, trace element and
875 mineral inclusions on high-pressure metamorphic overgrowth zircon in eclogite from Qinglongshan in
876 the Sulu terrane. Chinese Sci Bull 50: 459-465.
877 Li XP, Zheng YF, Wu YB, Chen FK, Gong B, Li YL (2004) Low-T eclogite in the Dabie terrane of China:
878 petrological and isotopic constraints on fluid activity and radiometric dating. Contrib Mineral Petrol 148:
879 443-470.
880 Liu DY, Jian P, Kröner A, Xu ST (2006a) Dating of prograde metamorphic events deciphered from episodic
881 zircon growth in rocks of the Dabie-Sulu UHP complex, China. Earth Planet Sci Lett 250: 650-666.
882 Liu FL, Liou JG (2011) Zircon as the best mineral for P–T–time history of UHP metamorphism: a review on
883 mineral inclusions and U–Pb SHRIMP ages of zircons from the Dabie–Sulu UHP rocks. J Asian Earth
884 Sci 40: 1-39.
885 Liu FL, Gerdes A, Liou JG, Xue HM, Liang FH (2006b) SHRIMP U-Pb zircon dating from Sulu-Dabie
886 dolomitic marble, eastern China: constraints on prograde, ultrahigh-pressure and retrograde metamorphic
887 ages. J Metamorphic Geol 24: 569-589.
888 Liu FL, Robinson PT, Gerdes A, Xue HM, Liu PH, Liou JG (2010b) Zircon U-Pb ages, REE concentrations and
889 Hf isotope compositions of granitic leucosome and pegmatite from the north Sulu UHP terrane in China:
890 constraints on the timing and nature of partial melting. Lithos 117: 247-268.
891 Liu FL, Robinson PT, Liu PH (2012) Multiple partial melting events in the Sulu UHP terrane: zircon U–Pb
892 dating of granitic leucosomes within amphibolite and gneiss. J Metamorphic Geol 30: 887-906.
893 Liu FL, Xu ZQ, Liou JG, Katayama I, Masago H, Maruyama S, Yang JS (2002) Ultrahigh-pressure mineral
894 inclusions in zircons from gneissic core samples of the Chinese Continental Scientific Drilling Site in
895 eastern China. Eur J Mineral 14: 499-512.

Liu XC, Jahn BM, Cui JJ, Li SZ, Wu YB, Li XH (2010a) Triassic retrograded eclogites and associated gneisses enclosed in Early Cretaceous gneissic granites from the Tongbai Complex, central China: constraints on the architecture of the HP/UHP Tongbai-Dabie-Sulu collision zone. Lithos 119: 211-237.

Liu XC, Jahn BM, Dong SW, Lou YX, Cui JJ (2008) High-pressure metamorphic rocks from Tongbaishan, central China: U-Pb and $^{40}Ar/^{39}Ar$ age constraints on the provenance of protoliths and timing of metamorphism. Lithos 105: 301-318.

Liu XC, Jahn BM, Liu DY, Dong SW, Li SZ (2004) SHRIMP U-Pb zircon dating of a metagabbro and eclogites from western Dabieshan (Hong'an Block), China, and its tectonic implications. Tectonophysics 394: 171-192.

Liu XC, Wu YB, Gao S, Wang J, Peng M, Gong HJ, Liu YS, Yuan HL (2011) Zircon U–Pb and Hf evidence for coupled subduction of oceanic and continental crust during the Carboniferous in the Huwan shear zone, western Dabie orogen, central China. J Metamorphic Geol 29: 233-249.

Liu YC, Li SG, Xu ST (2007) Zircon SHRIMP U-Pb dating for gneisses in northern Dabie high T/P metamorphic zone, central China: implications for decoupling within subducted continental crust. Lithos 96: 170-185.

Ludwig KR (2001a) User's Manual for Isoplot/Ex rev. 2.49: A Geochronological Toolkit for Microsoft Excel. Berkeley Geochronological Center Special Publication No. 1a.

Ludwig KR (2001b) SQUID 1.02, A User's Manual. Berkeley Geochronological Center Special Publication No. 2.

Martin L, Duchêne S, Deloule E, Vanderhaeghe O (2008) Mobility of trace elements and oxygen in zircon during metamorphism: consequences for geochemical tracing. Earth Planet Sci Lett 267: 161-174.

Mattinson JM (2005) Zircon U–Pb chemical abrasion ("CA-TIMS") method: combined annealing and multi-step partial dissolution analysis for improved precision and accuracy of zircon ages. Chem Geol 220: 47-66.

Monani S, Valley JW (2001) Oxygen isotope ratios of zircon: magma genesis of low $\delta^{18}O$ granites from the British Tertiary Igneous Province, western Scotland. Earth Planet Sci Lett 184: 377-392.

Niedermeier DRD, Putnis A, Geisler T, Golla-Schindler U, Putnis CV (2009) The mechanism of cation and oxygen isotope exchange in alkali feldspars under hydrothermal conditions. Contrib Mineral Petrol 157: 65-76.

Okay AI, Sengör AMC (1992) Evidence for intracontinental thrust-related exhumation of the ultra-high-pressure rocks in China. Geology 20: 411-414.

O'Neil JR, Taylor HP Jr (1967) The oxygen isotope and cation exchange chemistry of feldspars. Am Mineral 52: 1414-1437.

Page FZ, Kita NT, Valley JW (2010) Ion microprobe analysis of oxygen isotopes in garnets of complex chemistry. Chem Geol 270: 9-19.

Page FZ, Ushikubo T, Kita NT, Riciputi LR, Valley JW (2007a) High-precision oxygen isotope analysis of picogram samples reveals 2 μm gradients and slow diffusion in zircon. Am Mineral 92: 1772-1775.

Paton C, Woodhead JD, Hellstrom JC, Hergt JM, Greig A, Maas R (2010) Improved laser ablation U-Pb zircon geochronology through robust downhole fractionation correction. Geochem Geophys Geosyst 11, Q0AA06, doi: 10.1029/2009GC002618.

Peters TJ, Ayers JC, Gao S, Liu XM (2012) The origin and response of zircon in eclogite to metamorphism during the multi-stage evolution of the Huwan Shear Zone, China: insights from Lu–Hf and U–Pb isotopic and trace element geochemistry. Gondwana Res: in press, doi:10.1016/j.gr.2012.05.008.

Pidgeon RT, Furfaro D, Kennedy, AK, Nemchin AA, van Bronswjk W (1994) Calibration of zircon standards for the Curtin SHRIMP II. United States Geol Surv Circ 1107: 251 (abstr).

Roger F, Malavieille J, Leloup PH, Calassou S, Xu Z (2004) Timing of granite emplacement and cooling in the Songpan-Garzê Fold Belt (eastern Tibetan Plateau) with tectonic implications. J Asian Earth Sci 22: 465-481.

Russell AK, Kitajima K, Strickland A, Medaris LG Jr., Schulze DJ, Valley JW (2012) Eclogite-facies fluid infiltration: constraints from $\delta^{18}O$ zoning in garnet. Contrib Mineral Petrol: in press, doi: 10.1007/s00410-012-0794-9.

Rumble D, Giorgis D, Ireland T, Zhang ZM, Xu HF, Yui TF, Yang JS, Xu ZQ, Liou JG (2002) Low $\delta^{18}O$ zircons, U-Pb dating, and the age of the Qinglongshan oxygen and hydrogen isotope anomaly near Donghai in Jiangsu Province, China. Geochim Cosmochim Acta 66: 2299-2306.

Rumble D, Yui TF (1998) The Qinglongshan oxygen and hydrogen isotope anomaly near Donghai in Jiangsu Province, China. Geochim Cosmochim Acta 62: 3307-3321.

Savov IP, Leeman WP, Lee CT A, Shirey SB (2009) Boron isotopic variations in NW USA rhyolites: Yellowstone, Snake River Plain, Eastern Oregon. J Volcan Geotherm Res 188: 162-172.

954 Sheng YM, Zheng YF, Chen RX, Li QL, Dai MN (2012) Fluid action on zircon growth and recrystallization
955 during quartz veining within UHP eclogite: insights from U–Pb ages, O–Hf isotopes and trace elements.
956 Lithos 136-139: 126-144.
957 Sláma J, Košler J, Condon DJ, Crowley JL, Gerdes A, Hanchar JM, Horstwood MSA, Morris GA, Nasdala L,
958 Norberg N, Schaltegger U, Schoene B, Tubrett MN, Whitehouse MJ (2008) Plešovice zircon: a new
959 natural reference material for U–Pb and Hf isotopic microanalysis. Chem Geol 249: 1-35.
960 Stacey JS, Kramers JD (1975) Approximation of terrestrial lead isotope evolution by a two-stage model. Earth
961 Planet Sci Let 26: 207–221.
962 Stuart FM, Ellam RM, Harrop PJ, Fitton JG, Bell BR (2000) Constraints on mantle plumes from the helium
963 isotopic composition of basalts from the British Tertiary Igneous Province. Earth Planet Sci Lett 177: 273-
964 285.
965 Sun M, Chen NS, Zhao GC, Wilde SA, Ye K, Guo JH, Chen Y, Yuan C (2008) U-Pb zircon and Sm-Nd
966 isotopic study of the Huangtuling granulite, Dabie-Sulu belt, China: implication for the Paleoproterozoic
967 tectonic history of the Yangtze craton. Am J Sci 308: 469-483.
968 Sun WD, Williams IS, Li SG (2002) Carboniferous and Triassic eclogites in the western Dabie Mountains, east-
969 central China: evidence for protracted convergence of the North and South China Blocks. J Metamorphic
970 Geol 20: 873-886.
971 Tang J, Zheng YF, Gong B, Wu YB, Gao TS, Yuan HL, Wu FY (2008a) Extreme oxygen isotope signature of
972 meteoric water in magmatic zircon from metagranite in the Sulu Orogen, China: implications for
973 Neoproterozoic rift magmatism. Geochim Cosmochim Acta 72: 3139-3169.
974 Tang J, Zheng YF, Wu YB, Gong B, Liu XM (2007) Geochronology and geochemistry of metamorphic rocks in
975 the Jiaobei terrane: constraints on its tectonic affinity in the Sulu orogen. Precambrian Res 152: 48–82.
976 Tang J, Zheng YF, Wu YB, Gong B, Zha XP, Liu XM (2008b) Zircon U-Pb age and geochemical constraints on
977 the tectonic affinity of the Jiaodong terrane in the Sulu orogen, China. Precambrian Res 161: 389-418.
978 Taylor HP Jr (1986) Igneous rocks: II. isotopic case studies of circumpacific magmatism. In Stable Isotopes in
979 High Temperature Geological Processes (eds JW Valley, HP Taylor Jr, JR O'Neil). Mineralogical
980 Society of America, Washington, DC. Reviews in Mineralogy, v 16, pp 273-317.
981 Thirlwall MF, Gee MAM, Lowry D, Mattey DP, Murton BJ, Taylor RN (2006) Low $\delta^{18}O$ in the Icelandic
982 mantle and its origins: evidence from Reykjanes Ridge and Icelandic lavas. Geochim Cosmochim Acta
983 70: 993-1019.
984 Trail D, Bindeman IN, Watson EB, Schmitt AK (2009) Experimental calibration of oxygen isotope fractionation
985 between quartz and zircon. Geochim Cosmochim Acta 73: 7110-7126.
986 Trail D, Mojzsis SJ, Harrison TM, Schmitt AK, Watson EB, Young ED (2007) Constraints on Hadean zircon
987 protoliths from oxygen isotopes, Ti-thermometry, and rare earth elements. Geochem Geophys Geosyst 8,
988 Q06014, doi: 10.1029/2006GC001449.
989 Valley JW (2001) Stable isotope thermometry at high temperatures. In Stable Isotope Geochemistry (eds JW
990 Valley, DR Cole). Mineralogical Society of America/Geochemical Society, Washington, DC. Reviews in
991 Mineralogy and Geochemistry, v 43, pp 365-413.
992 Valley JW (2003) Oxygen isotopes in zircon. In Zircon (eds JM Hanchar, PWO Hoskin). Mineralogical Society
993 of America/Geochemical Society, Washington, DC. Reviews in Mineralogy and Geochemistry, v 53, pp
994 343-385.
995 Valley JW, Bindeman IN, Peck WH (2003) Empirical calibration of oxygen isotope fractionation in zircon.
996 Geochim Cosmochim Acta 67: 3257-3266.
997 Valley JW, Chiarenzelli JR, McLelland JM (1994) Oxygen isotope geochemistry of zircon. Earth Planet Sci Lett
998 126: 187-206.
999 Valley JW, Kitchen N, Kohn MJ, Niendorf CR, Spicuzza MJ (1995) UWG-2, a garnet standard for oxygen
1000 isotope ratios: strategies for high precision and accuracy with laser heating. Geochim Cosmochim Acta
1001 59: 5223-5231.
1002 Valley JW, Lackey JS, Cavosie AJ, Clechenko CC, Spicuzza MJ, Basei MAS, Bindeman IN, Ferreira VP, Sial
1003 AN, King EM, Peck WH, Sinha AK, Wei CS (2005) 4.4 billion years of crustal maturation: oxygen
1004 isotope ratios of magmatic zircon. Contrib Mineral Petrol 150: 561-580.
1005 Vielzeuf D, Champenois M, Valley JW, Brunet F, Devidal JL (2005) SIMS analysis of oxygen isotopes: matrix
1006 effects in Fe-Mg-Ca garnets. Chem Geol 223: 208-226.
1007 Wallis S, Tsuboi M, Suzuki K, Fanning M, Jiang LL, Tanaka T (2005) Role of partial melting in the evolution
1008 of the Sulu (eastern China) ultrahigh-pressure terrane. Geology 33: 129-132.
1009 Wang H, Wu YB, Gao S, Zhang HF, Liu XC, Gong HJ, Peng M, Wang J, Yuan HL (2011b) Silurian granulite-
1010 facies metamorphism, and coeval magmatism and crustal growth in the Tongbai orogen, central China.
1011 Lithos 125: 249–271

1012 Wang XC, Li ZX, Li XH, Li QL, Tang GQ, Zhang QR, Liu Y (2011a) Nonglacial origin for low-$\delta^{18}O$
1013 Neoproterozoic magmas in the South China Block: evidence from new in-situ oxygen isotope analysis
1014 using SIMS. Geology 39: 735-738.
1015 Wang XC, Li XH, Li ZX, Li QL, Tang GQ, Gap YY, Zhang QR, Liu Y (2012) Episodic Precambrian crust
1016 growth: evidence from U-Pb ages and Hf-O isotopes of zircon in the Nanhua Basin, central South China.
1017 Precambrian Res: in press, doi: 10.1016/j.precamres.2011.06.001.
1018 Watson EB, Cherniak DJ (1997) Oxygen diffusion in zircon. Earth Planet Sci Lett 148: 527-544.
1019 Watts KE, Bindeman IN, Schmitt AK (2011) Large-volume rhyolite genesis in caldera complexes of the Snake
1020 River Plain: insights from the Kilgore Tuff of the Heise Volcanic Field, Idaho, with comparison to
1021 Yellowstone and Bruneau–Jarbidge rhyolites. J Petrol 52: 857-890.
1022 Watts KE, Bindeman IN, Schmitt AK (2012) Crystal scale anatomy of a dying supervolcano: an isotope and
1023 geochronology study of individual phenocrysts from voluminous rhyolites of the Yellowstone caldera.
1024 Contrib Mineral Petrol 164: 45-67.
1025 Wiedenbeck M, Alle P, Corfu F, Griffin WL, Meier M, Oberli F, Von Quadt A, Roddick JC, Spiegel W (1995)
1026 Three natural zircon standards for U-Th-Pb, Lu-Hf, trace element and REE analyses. Geostandards
1027 Newsletter 19: 1–23.
1028 Williams IS (1998) U-Th-Pb geochronology by ion microprobe. In Applications of Microanalytical Techniques
1029 to Understanding Mineralizing Processes (eds MA McKibben, WC Shanks III, WI Ridley). Society of
1030 Economic Geologists, Littleton. Reviews in Economic Geology, v 7, pp 1-35.
1031 Woodhead J, Hellstrom J, Hergt J, Greig A, Maas R (2007) Isotopic and elemental imaging of geological
1032 materials by laser ablation Inductively Coupled Plasma mass spectrometry. J Geostand Geoanal Res 31,
1033 331-343.
1034 Woodhead J, Hergt J, Shelley M, Eggins S, Kemp R (2004) Zircon Hf-isotope analysis with an excimer laser,
1035 depth profiling, ablation of complex geometries, and concomitant age estimation. Chem Geol 209: 121–
1036 135.
1037 Wu YB, Gao S, Zhang HF, Yang SH, Jiao WF, Liu YS, Yuan HL (2008a) Timing of UHP metamorphism in the
1038 Hong'an area, western Dabie Mountains, China: evidence from zircon U-Pb age, trace element and Hf
1039 isotope composition. Contrib Mineral Petrol 155: 123-133.
1040 Wu YB, Zheng YF, Gao S, Jiao WF, Liu YS (2008b) Zircon U–Pb age and trace element evidence for
1041 Paleoproterozoic granulite-facies metamorphism and Archean crustal rocks in the Dabie Orogen. Lithos
1042 101: 308-322.
1043 Wu YB, Hanchar JM, Gao S, Sylvester PJ, Tubrett M, Qiu HN, Wijbrans JR, Brower FM, Yang SH, Yang QJ,
1044 Liu YS, Yuan HL (2009) Age and nature of eclogites in the Huwan shear zone, and the multi-stage
1045 evolution of the Qinling-Dabie-Sulu orogen, central China. Earth Planet Sci Lett 277: 345-354.
1046 Wu YB, Zheng YF, Tang J, Gong B, Zhao ZF, Liu XM (2007) Zircon U–Pb dating of water–rock interaction
1047 during Neoproterozoic rift magmatism in South China. Chem Geol 246: 65-86.
1048 Wu YB, Zheng YF, Zhao ZF, Gong B, Liu XM, Wu FY (2006) U-Pb, Hf and O isotope evidence for two
1049 episodes of fluid-assisted zircon growth in marble-hosted eclogites from the Dabie orogen. Geochim
1050 Cosmochim Acta 70: 3743-3761.
1051 Xia QK, Deloule E, Wu YB, Chen DG, Cheng H (2002) Oxygen isotopic compositions of zircons from
1052 pyroxenite of Daoshichong, Dabieshan: implications for crust-mantle interaction. Chinese Sci Bull 47:
1053 1466-1469.
1054 Xia QX, Zheng YF, Yuan HL, Wu FY (2009) Contrasting Lu-Hf and U-Th-Pb isotope systematics between
1055 metamorphic growth and recrystallization of zircon from eclogite-facies metagranite in the Dabie orogen,
1056 China. Lithos 112: 477-496.
1057 Xia QX, Zheng YF, Zhou LG (2008) Dehydration and melting during continental collision; constraints from
1058 element and isotope geochemistry of low-T/UHP granitic gneiss in the Dabie Orogen. Chem Geol 247:
1059 36-65.
1060 Xia QX, Zheng YF, Hu ZC (2010) Trace elements in zircon and coexisting minerals from low-T/UHP
1061 metagranite in the Dabie orogen: implications for action of supercritical fluid during continental
1062 subduction-zone metamorphism. Lithos 114: 385-412.
1063 Xiao YL, Hoefs J, van den Kerkhof AM, Li SG (2001) Geochemical constraints of the eclogite and granulite
1064 facies metamorphism as recognized in the Raobazhai complex from North Dabie Shan, China. J
1065 Metamorphic Geol 19: 3-19.
1066 Xiao YL, Hoefs J, van den Kerkhof AM, Simon K, Fiebig J, Zheng YF (2002) Fluid evolution during HP and
1067 UHP metamorphism in Dabie Shan, China: constraints from mineral chemistry, fluid inclusions and
1068 stable isotopes. J Petrol 43: 1505-1527.
1069 Xiao YL, Zhang ZM, Hoefs J, van den Kerkhof A (2006) Ultrahigh pressure metamorphic rocks from the
1070 Chinese Continental Scientific Drilling Project; II, Oxygen isotope and fluid inclusion distributions
1071 through vertical sections. Contrib Mineral Petrol 152: 443-458.

1072 Xie Z, Zheng YF, Zhao ZF, Wu YB, Wang ZR, Chen JF, Liu XM, Wu FY (2006) Mineral isotope evidence for
1073 the contemporaneous process of Mesozoic granite emplacement and gneiss metamorphism in the Dabie
1074 orogen. Chem Geol 231: 214-235.
1075 Yan DP, Zhou MF, Wei GQ, Gao JF, Liu SF, Xu P, Shi XY (2008) The Pengguan tectonic dome of Longmen
1076 Mountains, Sichuan Province: Mesozoic denudation of a Neoproterozoic magmatic arc-basin system. Sci
1077 China (Series D, Earth Sci) 51: 1545-1559.
1078 Ye K, Yao YP, Katayama I, Cong BL, Wang QC, Maruyama S (2000) Large areal extent of ultrahigh-pressure
1079 metamorphism in the Sulu ultrahigh-pressure terrane of East China: new implications from coesite and
1080 omphacite inclusions in zircon of granitic gneiss. Lithos 52: 157-164.
1081 Yui TF, Rumble III D, Lo CH (1995) Unusually low $\delta^{18}O$ ultra-high-pressure metamorphic rocks from the Su-
1082 Lu Terrain, eastern China. Geochim Cosmochim Acta 59: 2859-2864.
1083 Zhang SB, Zheng YF, Zhao ZF, Wu YB, Yuan HL, Wu FY (2008) Neoproterozoic anatexis of Archean
1084 lithosphere: geochemical evidence from felsic to mafic intrusives at Xiaofeng in the Yangtze George,
1085 South China. Precambrian Res 163: 210-238.
1086 Zhang SB, Zheng YF, Zhao ZF, Wu YB, Yuan HL, Wu FY (2009) Origin of TTG-like rocks from anatexis of
1087 ancient lower crust: geochemical evidence from Neoproterozoic granitoids in South China. Lithos 113:
1088 347-368.
1089 Zhao ZF, Zheng YF (2002) Calculation of oxygen isotope fractionation in magmatic rocks. Chem Geol 193: 59-
1090 80.
1091 Zhao ZF, Zheng YF, Wei CS, Wu YB (2004) Zircon isotope evidence for recycling of subducted continental
1092 crust in post-collisional granitoids from the Dabie terrane in China. Geophys Res Lett 31: L22602 1-4.
1093 Zhao ZF, Zheng YF, Wei CS, Wu YB (2007) Post-collisional granitoids from the Dabie orogen in China: zircon
1094 U–Pb age, element and O isotope evidence for recycling of subducted continental crust. Lithos 93: 248-
1095 272.
1096 Zhao ZF, Zheng YF, Wei CS, Wu YB, Chen FK, Jahn BM (2005) Zircon U-Pb age, element and C-O isotope
1097 geochemistry of post-collisional mafic-ultramafic rocks from the Dabie orogen in east-central China.
1098 Lithos 83: 1-28.
1099 Zhao ZF, Zheng YF, Zhang J, Dai LQ, Li QL, Liu XM (2012) Syn-exhumation magmatism during continental
1100 collision: evidence from alkaline intrusives of Triassic age in the Sulu orogen. Chem Geol 328: 70-88.
1101 Zheng YF (1993a) Calculation of oxygen isotope fractionation in anhydrous silicate minerals. Geochim
1102 Cosmochim Acta 57: 1079-1091.
1103 Zheng YF (1993b) Calculation of oxygen isotope fractionation in hydroxyl-bearing silicates. Earth Planet Sci
1104 Lett 120: 247-263.
1105 Zheng YF, Chen RX, Zhao ZF (2009) Chemical geodynamics of continental subduction-zone metamorphism:
1106 insights from studies of the Chinese Continental Scientific Drilling (CCSD) core samples.
1107 Tectonophysics 475: 327-358.
1108 Zheng YF, Fu B, Gong B, Li L (2003) Stable isotope geochemistry of ultrahigh pressure metamorphic rocks
1109 from the Dabie-Sulu orogen in China: implications for geodynamics and fluid regime. Earth–Sci Rev 62:
1110 105-161.
1111 Zheng YF, Fu B, Gong B, Li S (1996) Extreme ^{18}O depletion in eclogite from the Su-Lu terrane in East China.
1112 Eur J Mineral 8: 317-323.
1113 Zheng YF, Fu B, Gong B, Xiao YL, Wei CS, Li SG (1998b) Oxygen isotope constraints on fluid flow during
1114 eclogitization in the Sulu terrane. Prog Nat Sci 8: 98-105.
1115 Zheng YF, Fu B, Li YL, Xiao YL, Li SG (1998a) Oxygen and hydrogen isotope geochemistry of ultrahigh
1116 pressure eclogites from the Dabie Mountains and the Sulu terrane. Earth Planet Sci Lett 155: 113-129.
1117 Zheng YF, Fu B, Xiao YL, Li YL, Gong B (1999) Hydrogen and oxygen isotope evidence for fluid-rock
1118 interactions in the stages of pre- and post-UHP metamorphism in the Dabie Mountains. Lithos 46: 677-
1119 693.
1120 Zheng YF, Gong B, Zhao ZF, Wu YB, Chen FK (2008) Zircon U-Pb age and O isotope evidence for
1121 Neoproterozoic low-$\delta^{18}O$ magmatism during supercontinental rifting in South China: implications for the
1122 snowball Earth event. Am J Sci 308: 484-516.
1123 Zheng YF, Wu YB, Chen FK, Gong B, Li L, Zhao ZF (2004) Zircon U-Pb and oxygen isotope evidence for a
1124 large-scale ^{18}O depletion event in igneous rocks during the Neoproterozoic. Geochim Cosmochim Acta
1125 68: 4145-4165.
1126 Zheng YF, Wu YB, Gong B, Chen RX, Tang J, Zhao ZF (2007a) Tectonic driving of Neoproterozoic
1127 glaciations: evidence from extreme oxygen isotope signature of meteoric water in granite. Earth Planet
1128 Sci Lett 256: 196-210.
1129 Zheng YF, Zhang SB, Zhao ZF, Wu YB, Li XH, Li ZX, Wu FY (2007b) Contrasting zircon Hf and O isotopes
1130 in the two episodes of Neoproterozoic granitoids in South China: implications for growth and reworking
1131 of continental crust. Lithos 96: 127-150.

Zhou JB, Wilde SA, Zhao GC, Zheng CQ, Jin W, Zhang XZ, Cheng H (2008) SHRIMP U-Pb zircon dating of the Neoproterozoic Penglai Group and Archean gneisses from the Jiaobei Terrane, North China, and their tectonic implications. Precambrian Res 160: 323-340.

Zhou MF, Yan DP, Kennedy AK, Li YQ, Ding J (2002) SHRIMP U-Pb zircon geochronological and geochemical evidence for Neoproterozoic arc-magmatism along the western margin of the Yangtze Block, South China. Earth Planet Sci Lett 196: 51-67.

Zhou MF, Yan DP, Wang CL, Qi L, Kennedy AK (2006) Subduction-related origin of the 750 Ma Xuelongbao adakitic complex (Sichuan Province, China): implications for the tectonic setting of the giant Neoproterozoic magmatic event in South China. Earth Planet Sci Lett 248: 286-300.

FIGURE CAPTIONS

Figure 1. Geological maps showing sample locations. The inset in (a) shows the location of the Qingling-Tongbai-Dabie-Sulu orogenic belt between the North China Block and the South China Block, east-central China, and the simplified geological maps show: (a) the Sulu terrane; (b) the Dabie terrane (including the Hong'an area or W. Dabie) and (c) the Tongbai terrane. Key localities include: ZBZ – Zaobuzhen, Sulu; BXL – Bixiling, HZ – Huangzhen, HLS – Huilanshan, LZG – Luzhenguan, from Dabie, and CCSD-MH – Chinese Continental Scientific Drilling – Main Hole, Sulu. See main text for abbreviations for faults and tectonic units. A schematic geological map of Longmenshan in southwestern China is shown in (d) and its geographical position in the inset (figure courtesy of Y.T. Tian), modified after CIGMR (2004) and Roger et al. (2004). Abbreviations in (d): BC, Baoxing Complex, PC, Pengguan Complex, XC, Xuelongbao Complex, KC, Kangding Complex, and in the inset: SG, Songpan-Garzê belt, BH, Bayan Har terrane, Yi, Yidun or Litang-Batang terrane, Si, Simao terrane, IND, Indochina. Note that three samples (#70-72) from South Qinling and two other miscellaneous samples (#78 & #79) from the South China and North China blocks (see Electronic supplementary materials S1) are not shown on the maps.

Figure 2. Representative CL images showing zircons in rocks from the Tongbai-Dabie-Sulu orognic belt: (a) grain no. 5, sample #2; (b) grain no. 3, sample #3; (c) grain no. 6, sample #20; (d) grain no. 15, sample #53; (e) grain no. 2, sample #73; (f) grain no. 3, sample #77; (g & h) grain nos. 1 & 6, sample #50; and (i & j) grain nos. 13 & 14, sample #30. Solid ellipses denote SIMS dating spots and dashed ones $^{18}O/^{16}O$-analysis sites; circles represent LA-ICP-MS dating sites. Note that the zircons (a) to (d) have contrasting $\delta^{18}O$ values between Neoproterozoic "igneous" zircon cores and Triassic metamorphic zircon rims, varying by up to 13.3‰, whereas the zircons (e) to (j) are relatively homogeneous in $\delta^{18}O$, and that six additional analyses of the zircon (d) for $^{18}O/^{16}O$ were performed after repolishing. Scale bars are 20 μm. The U-Pb ages and oxygen values are presented for each analytical site.

Figure 3. Plot of $\delta^{18}O$(Min = mineral) *versus* $\delta^{18}O$(Grt = garnet) for some of the investigated samples from the Tongbai-Dabie-Sulu orogenic belt, analyzed by laser fluorination. Average $\delta^{18}O$ for metamorphic zircons ($n \geq 4$) from 5 rock samples analyzed by ion microprobe is also plotted; 2 SD ≤ ±0.8‰, comparable to the analytical precision, ≤ ±0.4‰. Note that all data points fall between $\Delta^{18}O$(Min-Grt) = 1 and 0. Abbreviations: Omph, omphacite; Zo, zoisite; Amph, amphibole; and M-Zrn, metamorphic zircon. $\delta^{18}O$(Grt) for samples (#3 & #19) was taken from Zheng et al. (1998b) and Fu et al. (1999), respectively. See Electronic supplementary materials S1 for sample numbers.

Figure 4. Oxygen isotope ratios measured in situ by ion microprobe for zircons in rocks fom the Qinling-Tongbai-Dabie-Sulu orogenic belt and adjacent areas. Vertical lines at 4.7‰ and 5.9‰ define the normal $\delta^{18}O$ range for zircon in high temperature equilibrium with mantle compositions. Abbreviations: Zrn, zircon; TDS, Tongbai-Dabie-Sulu; NCB, North China Block; SCB, South China Block. The numbers (1 to 79) along the right vertical axis denote samples as listed in Electronic supplementary materials S1.

Figure 5. Concordia diagrams for zircons in selected rock samples from the Qinling-Tongbai-Dabie-Sulu orogenic belt and adjacent areas, analyzed by: (a) ion microprobe (see Electronic supplementary materials or ESM S4), "false" discordia intercept ages for a total of 19 samples are given; and (b to f) laser ablation inductively coupled plasma mass spectrometry (ESM S5). Data-point error ellipses are 2 standard errors.

Figure 6. Plots of in situ zircon $\delta^{18}O$ data *versus* U-Th-Pb results for all the investigated samples from the Qinling-Tongbai-Dabie-Sulu orogenic belt and adjacent areas. (a) $\delta^{18}O$ *versus* $^{206}Pb/^{238}U$ or $^{207}Pb/^{206}Pb$ age (≥ 1200 Ma); (b & c) $\delta^{18}O$ *versus* Th/U for zircons with ages of 800-600 Ma and 245-200 Ma, respectively. Abbreviations: TDS, Qinling-Tongbai-Dabie-Sulu; SCB, South China Block; NCB, North China Block; SIMS, ion microprobe; and ICP-MS, (laser ablation) inductively coupled plasma mass spectrometry. Age data sources: Liu et al. (2004, 2008, 2010a), Wallis et al. (2005), Cui et al. (2012), Hu et al. (2012) and this study.

Figure 7. Plots of in situ zircon $\delta^{18}O$ *versus* age for selected samples from the Tongbai-Dabie-Sulu orogenic belt: (a) Sulu; (b) Dabie and Hong'an (or W. Dabie); and (c) Tongbai.

Figure 8. δ–δ diagrams. (a) Plot of average $\delta^{18}O$ of Triassic metamorphic zircons (M-Zrn; 245-200 Ma) *versus* $\delta^{18}O$ of Neoproterozoic "igneous" zircons (I-Zrn; 800-600 Ma) from the same metaigneous rock samples at Tongbai-Dabie-Sulu. Number of individual analyses for average $\delta^{18}O$ calculation is ≥2. Four groups (I to IV) of host metaigneous rocks have been identified: Group I,

$\delta^{18}O$(M-Zrn) ≈ $\delta^{18}O$(I-Zrn), 4.0‰ to 6.5‰; Group II, $\delta^{18}O$(M-Zrn), 0 to 4.0‰ and $\delta^{18}O$(I-Zrn), 4.0‰ to 6.5‰; Group III, $\delta^{18}O$(M-Zrn) ≈ $\delta^{18}O$(I-Zrn), 0 to 4.0‰; Group IV, $\delta^{18}O$(M-Zrn) << $\delta^{18}O$(I-Zrn), –9.9‰ to 4.0‰. See Electronic supplementary materials S1 for sample details. (b) Plot of average $\delta^{18}O$ (±2 SD) for igneous zircon rims (Zrn-rim) *versus* $\delta^{18}O$ for igneous zircon cores (Zrn-core), from individual rhyolitic samples from Yellowstone (Bindeman et al. 2008a). Three groups (A, B & C) of host rhyolites have been identified. The numbers are ages (in Ma) of the rock samples. Uncertainties are plotted as ±2 SD for multiple spot analyses and in many cases represent real sample-to-sample variability in $\delta^{18}O$.

ELECTRONIC SUPPLEMENTARY MATERIALS S1 to S6.

(in a separate Excel file)

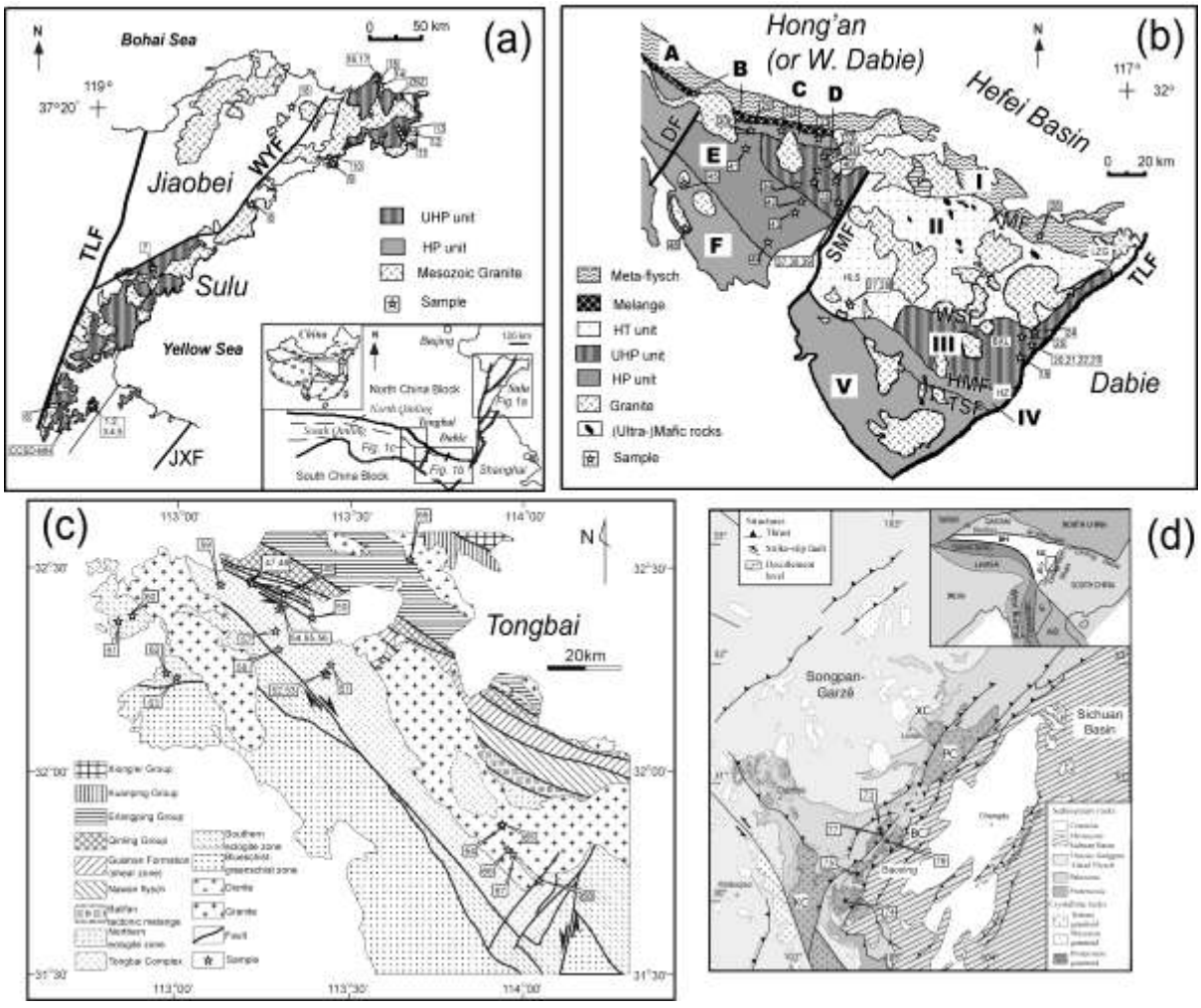

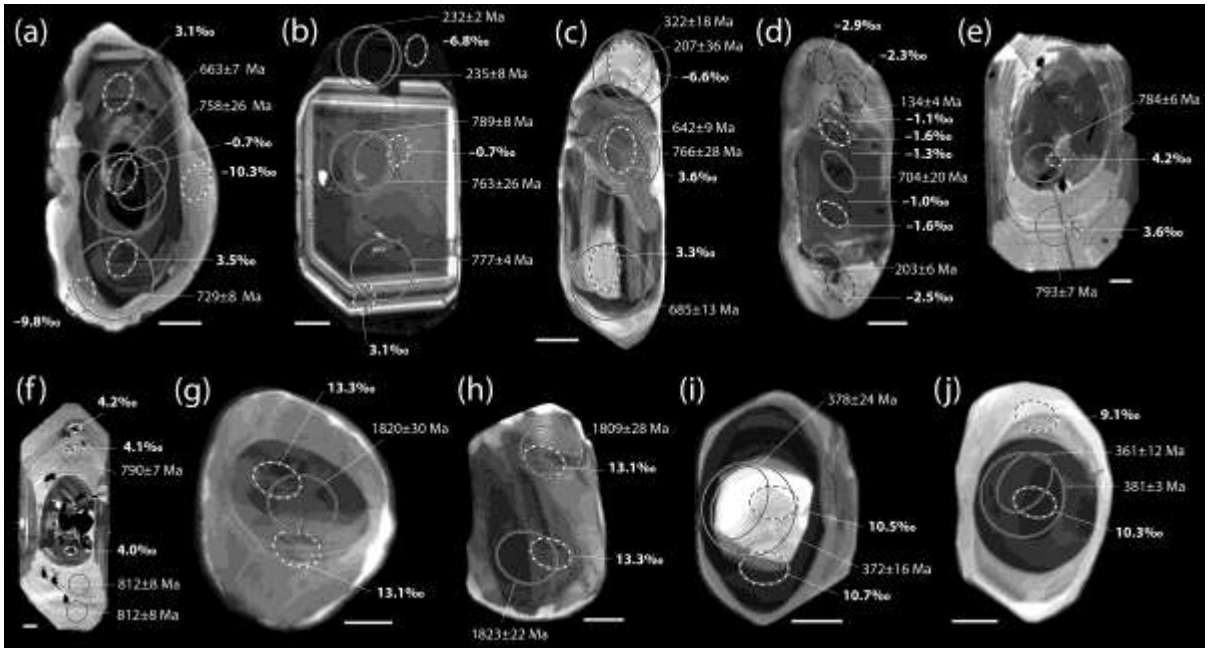
(a)
3.1‰
663±7 Ma
758±26 Ma
-0.7‰
-10.3‰
3.5‰
729±8 Ma
-9.8‰
(b)
232±2 Ma
-6.8‰
235±8 Ma
789±8 Ma
-0.7‰
763±26 Ma
777±4 Ma
3.1‰
(c)
322±18 Ma
207±36 Ma
-6.6‰
642±9 Ma
766±28 Ma
3.6‰
3.3‰
685±13 Ma
(d)
-2.9‰
-2.3‰
134±4 Ma
-1.1‰
-1.6‰
-1.3‰
704±20 Ma
-1.0‰
-1.6‰
203±6 Ma
-2.5‰
(e)
784±6 Ma
4.2‰
3.6‰
793±7 Ma
(f)
4.2‰
4.1‰
790±7 Ma
4.0‰
812±8 Ma
812±8 Ma
(g)
13.3‰
1820±30 Ma
13.1‰
(h)
1809±28 Ma
13.1‰
13.3‰
1823±22 Ma
(i)
378±24 Ma
10.5‰
372±16 Ma
10.7‰
(j)
9.1‰
361±12 Ma
381±3 Ma
10.3‰

1221

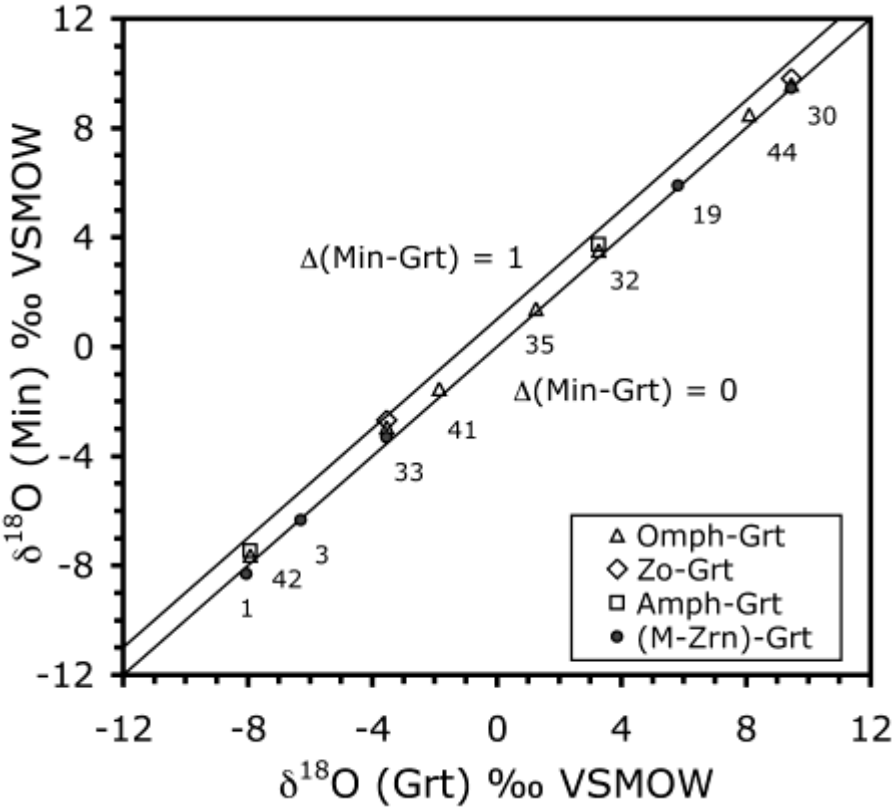
12
8
4
0
-4
-8
-12
-12
-8
-4
0
4
8
12
δ18O (Min) ‰ VSMOW
δ18O (Grt) ‰ VSMOW
Δ(Min-Grt) = 1
Δ(Min-Grt) = 0
30
44
19
32
35
41
33
3
42
1
Omph-Grt
Zo-Grt
Amph-Grt
(M-Zrn)-Grt

1222

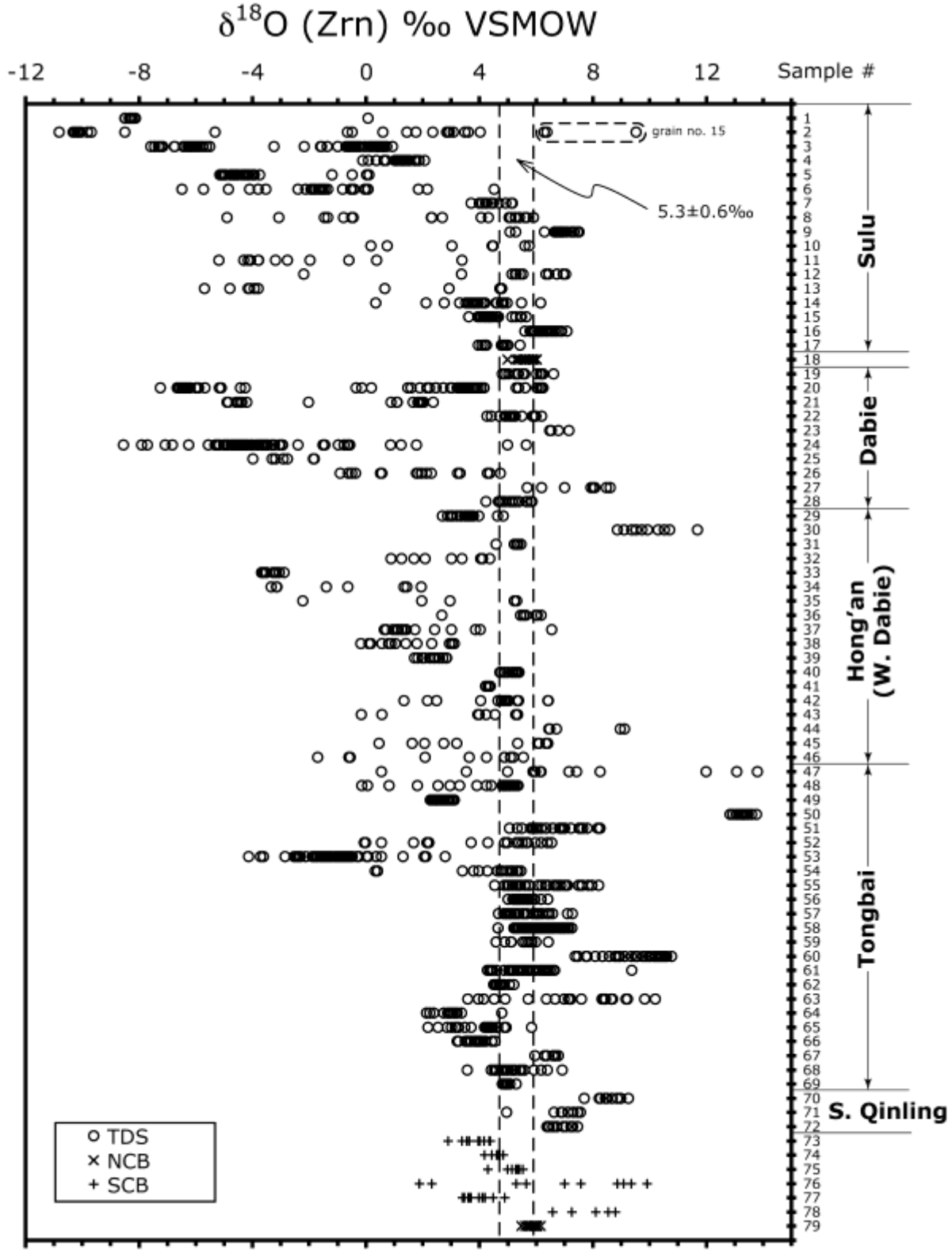
δ18O (Zrn) ‰ VSMOW
-12
-8
-4
0
4
8
12
Sample #
grain no. 15
5.3±0.6‰
Sulu
Dabie
Hong'an
(W. Dabie)
Tongbai
S. Qinling
TDS
NCB
SCB

1223

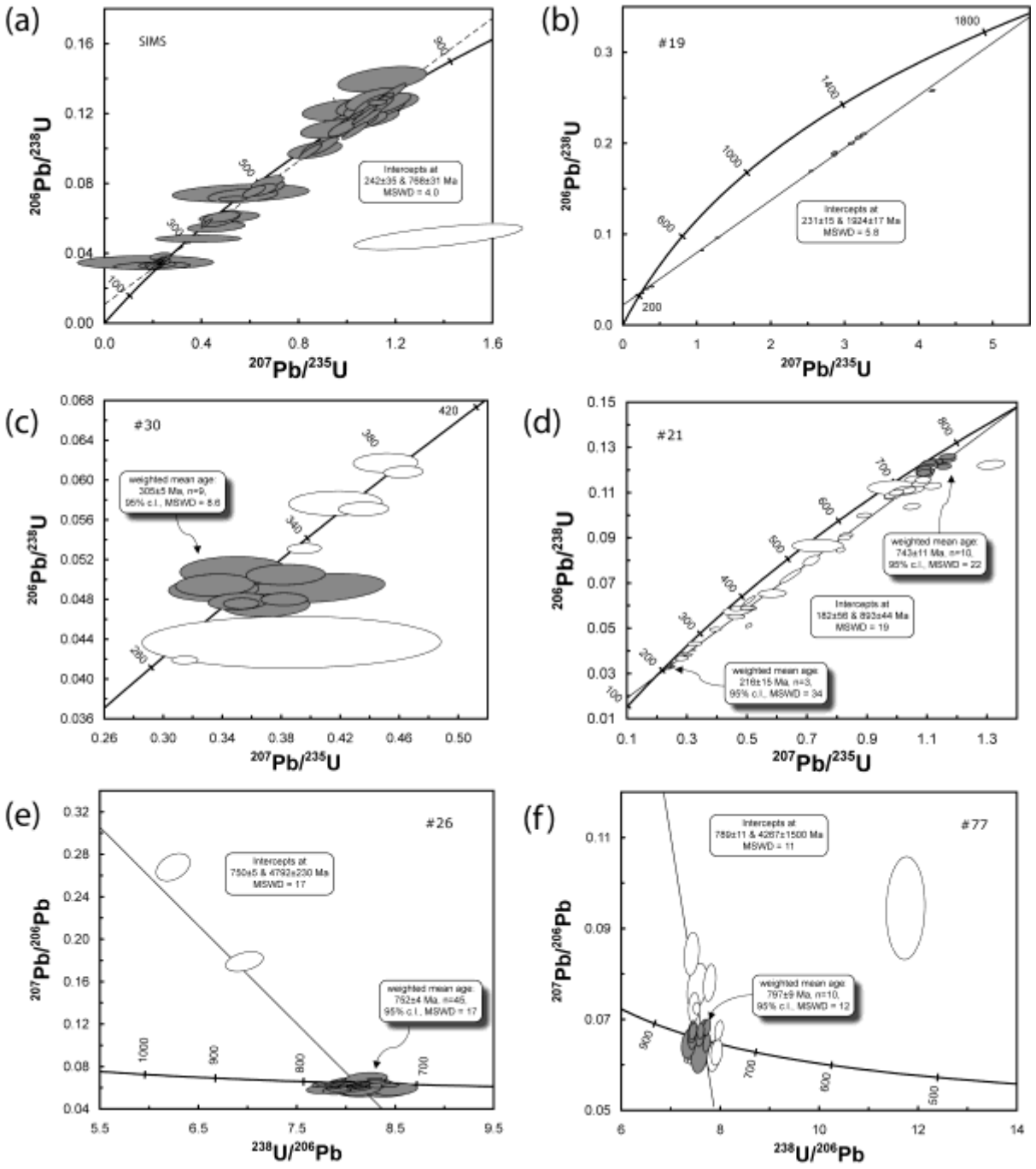
(a)
SIMS
Intercepts at
242±35 & 768±31 Ma
MSWD = 4.0
$^{206}Pb/^{238}U$
$^{207}Pb/^{235}U$
(b)
#19
Intercepts at
231±15 & 1824±17 Ma
MSWD = 5.8
$^{206}Pb/^{238}U$
$^{207}Pb/^{235}U$
(c)
#30
weighted mean age:
305±5 Ma, n=9,
95% c.l., MSWD = 5.6
$^{206}Pb/^{238}U$
$^{207}Pb/^{235}U$
(d)
#21
weighted mean age:
743±11 Ma, n=10,
95% c.l., MSWD = 22
Intercepts at
182±56 & 893±44 Ma
MSWD = 19
weighted mean age:
216±15 Ma, n=3,
95% c.l., MSWD = 34
$^{206}Pb/^{238}U$
$^{207}Pb/^{235}U$
(e)
#26
Intercepts at
750±5 & 4792±230 Ma
MSWD = 17
weighted mean age:
752±4 Ma, n=46,
95% c.l., MSWD = 17
$^{207}Pb/^{206}Pb$
$^{238}U/^{206}Pb$
(f)
#77
Intercepts at
789±11 & 4287±1500 Ma
MSWD = 11
weighted mean age:
797±9 Ma, n=10,
95% c.l., MSWD = 12
$^{207}Pb/^{206}Pb$
$^{238}U/^{206}Pb$

1224

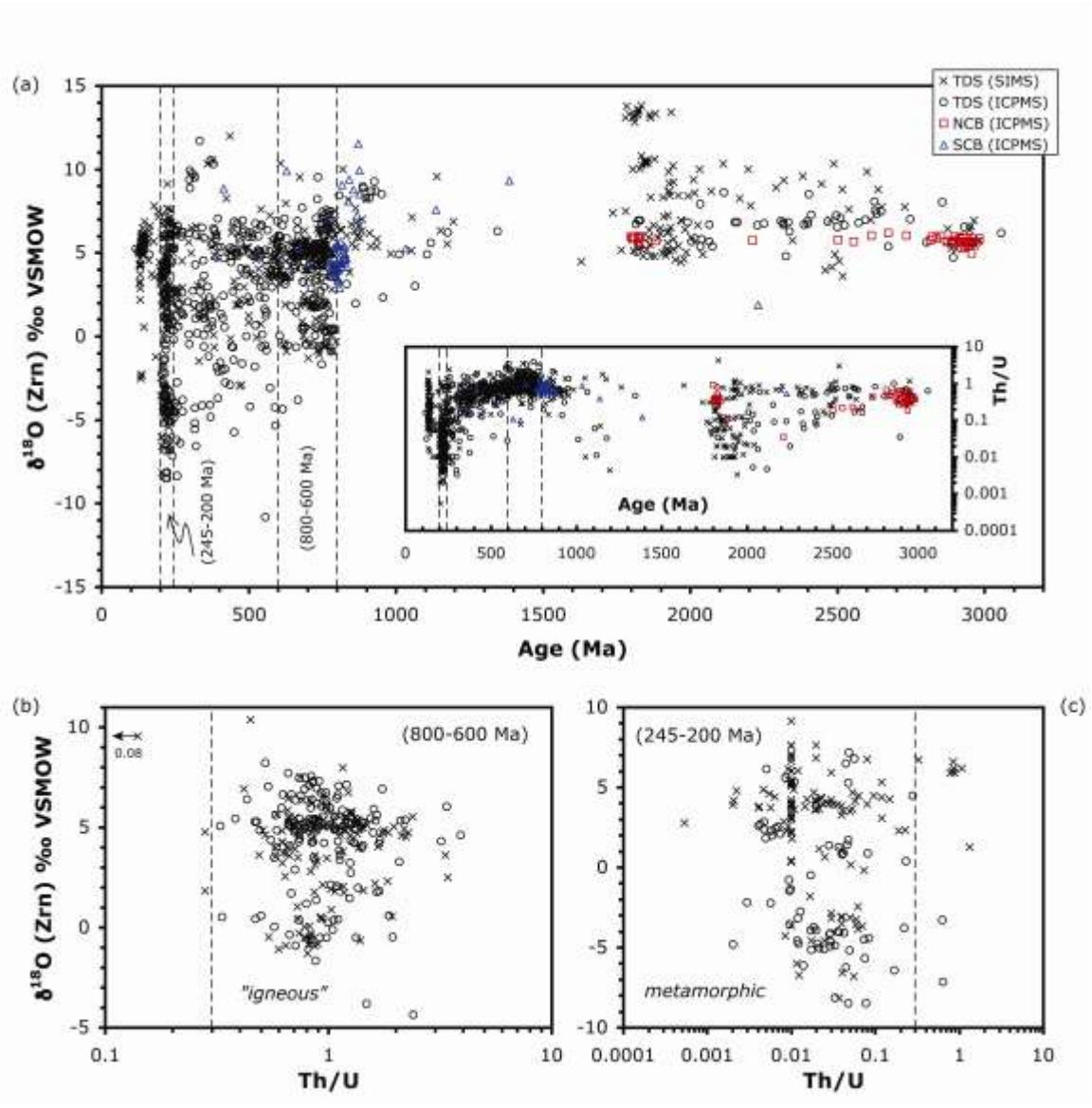
(a)
TDS (SIMS)
TDS (ICPMS)
NCB (ICPMS)
SCB (ICPMS)
δ18O (Zrn) ‰ VSMOW
Age (Ma)
(245-200 Ma)
(800-600 Ma)
Th/U
(b)
(800-600 Ma)
0.08
"igneous"
(c)
(245-200 Ma)
metamorphic

1225

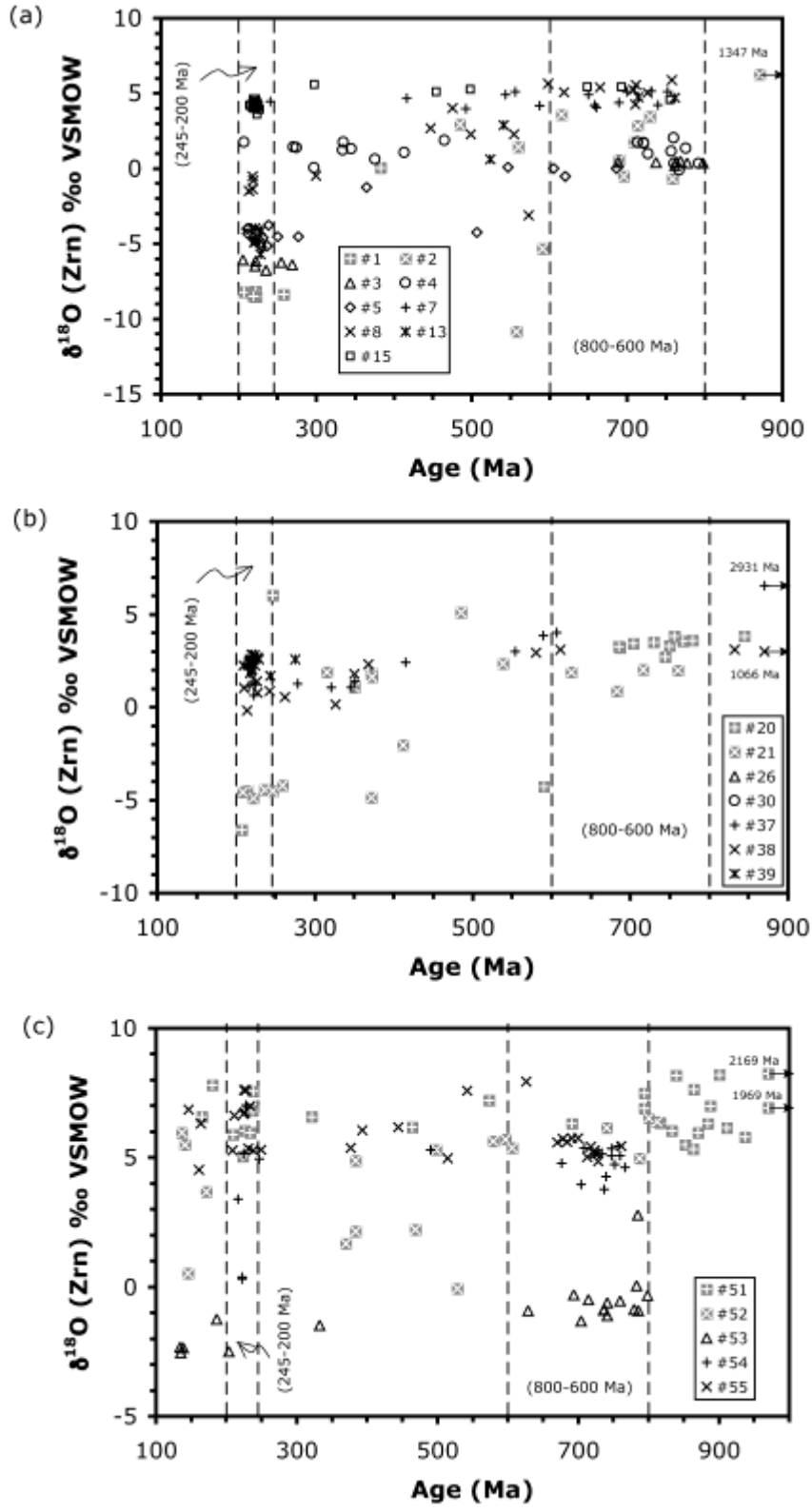
(a)
δ18O (Zrn) ‰ VSMOW
Age (Ma)
(245-200 Ma)
(800-600 Ma)
1347 Ma
#1 #2
#3 #4
#5 #7
#8 #13
#15
(b)
δ18O (Zrn) ‰ VSMOW
Age (Ma)
(245-200 Ma)
(800-600 Ma)
2931 Ma
1066 Ma
#20
#21
#26
#30
#37
#38
#39
(c)
δ18O (Zrn) ‰ VSMOW
Age (Ma)
(245-200 Ma)
(800-600 Ma)
2169 Ma
1969 Ma
#51
#52
#53
#54
#55

1226

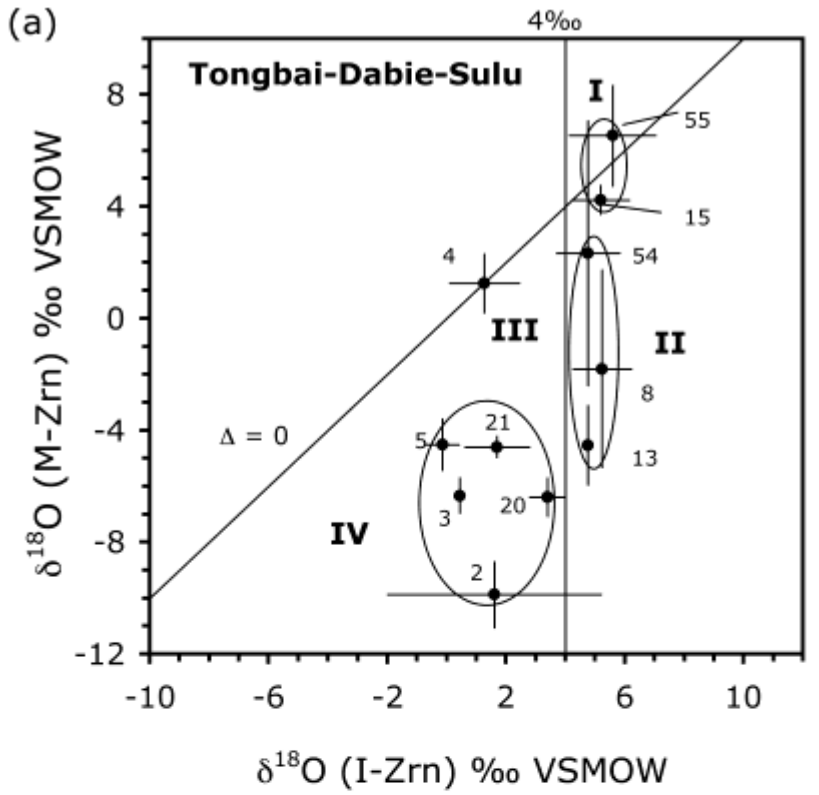
(a)
Tongbai-Dabie-Sulu
4‰
I
II
III
IV
55
15
54
8
13
4
21
5
3
20
2
Δ = 0
δ18O (M-Zrn) ‰ VSMOW
δ18O (I-Zrn) ‰ VSMOW
8
4
0
-4
-8
-12
-10
-6
-2
2
6
10

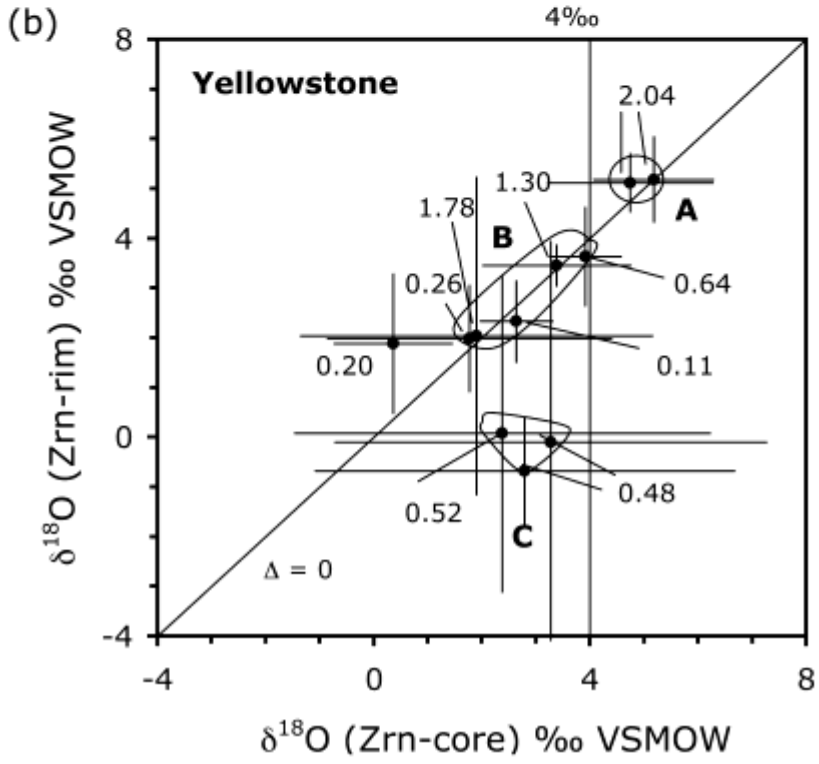
(b)
Yellowstone
4‰
2.04
1.30
1.78
A
B
0.26
0.64
0.20
0.11
0.48
0.52
C
Δ = 0
δ18O (Zrn-rim) ‰ VSMOW
δ18O (Zrn-core) ‰ VSMOW
8
4
0
-4
-4
0
4
8

1227